Dynamical Climatology

The sensitivity of the Saharan region in a general circulation model

by

W.M.Cunnington and P.R.Rowntree

DCTN 19 February 1985

Meteorological Office (Met. O. 20)
London Road
Bracknell
Berkshire RG12 2SZ

DYNAMICAL CLIMATOLOGY TECHNICAL NOTE NO. 19

THE SENSITIVITY OF THE SAHARAN REGION IN A GENERAL CIRCULATION MODEL

by

W M Cunnington and P R Rowntree

This paper, which is a considerably extended version of Technical Note II/205, has been submitted for publication in the Quart. J. Roy. Met. Soc.

Met O 20 (Dynamical
Climatology Branch)
Meteorological Office
London Road
Bracknell
Berkshire, U.K. RG12 2SZ

February 1985

THE SENSITIVITY OF THE SAHARAN REGION IN A GENERAL CIRCULATION MODEL

by W. M. Cunnington and P. R. Rowntree

U.K. Meteorological Office

Summary

The sensitivity of an atmospheric general circulation model to changes in atmospheric water content, soil moisture content, radiation scheme and albedo have been investigated using the U.K. Meteorological Office global 11-layer model. Previous integrations starting with a moist atmosphere and dry soil over the Saharan region had produced excessive rainfall in the desert region. It is shown that a dry Sahara with realistic circulation patterns is simulated only by starting with a realistically dry atmosphere and dry soil and by using a radiation scheme with longwave radiation dependent on atmospheric water vapour content. With a moist atmosphere, introduced either initially or by rapid evaporation from a wet soil, or by using a radiation scheme without water vapour dependence, there is increased net downward radiation which enhances ascent and convective activity and leads eventually to excessive rainfall in the desert region with 700 mb westerly winds at 5° - 15°N associated with a cyclonic circulation over the Saharan region which draws in moist air from the south. The use of more realistic albedos tends to transfer rainfall from regions of higher albedo (eg deserts) to regions of lower albedo (eg forests).

1. Introduction

In his Royal Meteorological Society Symons Memorial Lecture for 1974, Charney (1975) proposed a model for the maintenance of deserts. This depends upon a feedback mechanism involving radiation, subsidence, and albedo. A lack of rainfall results in a lack of vegetation giving a higher surface albedo which leads to a net radiative heat loss at the top of the atmosphere. This encourages subsidence of dry air aloft with a consequent reduction in precipitation so maintaining the desert. The hypothesis was subsequently tested in numerical simulations with a general circulation model (Charney et al., 1977) in which increases in the albedo from 0.14 to 0.35 over desert regions were accompanied by substantial decreases of rainfall. Subsequent experiments using a different general circulation model (Chervin 1979) in which the albedo over the Sahara desert was increased gave similar results. Recently, Sud and Fennessy (1982) carried out numerical experiments similar to those of Charney, but with a different model, which again support Charney's hypothesis.

Another mechanism for the persistence of anomalies in surface aridity was discussed by Walker and Rowntree (1977), using a simplified limited-area tropical version of the 11-layer model used in this paper. They showed that if land corresponding to the Saharan region was initialised either moist or dry it maintained this initial state over a period of at least some weeks, supporting the idea that surface aridity is an important factor in the persistence of deserts.

Walker and Rowntree pointed out the marked persistence of dry and wet spells in the Sahel region of west Africa, especially the dry period commencing in the mid 1960's. This dry period still continues in 1984 with an increase in intensity from about 1980 onwards so that, according to the analysis by Dennett et al (1985), the June-September rainfalls for 1982 and 1983 were the lowest since before 1941 for the area in 10° - 20°N from 17°E to the west coast (see also Nicholson (1981) and Lamb (1983)). Palaeoclimatic studies of the Sahara indicate much larger variations in the climate of North Africa over the last 20,000 years (e.g. Street and Grove, 1979) with drier conditions than now about 14,000 yr. B.P. (years before present) and much wetter conditions about 9000 yr B.P.

Although the work reported in this paper is, in the first instance, directed at understanding model sensitivity, the results may, as discussed in section 4, also provide evidence on possible mechanisms involved in these Sahelian and Saharan climate variations. The results obtained will therefore be compared, where possible, with variations observed in association with the Sahel drought.

Previous experiments with the 11-layer model (see, for example, Fig 2(a)) had shown that excessive rainfall is simulated over the Sahara in July, the tropical wet region extending beyond its climatological northern limit of near 18°N to about 25° -30°N. The initial atmospheric conditions for these experiments were taken from a model with the soil moisture content specified at a high value so that the atmosphere, even over deserts, had become unrealistically moist. Although the 11-layer model has interactive soil moisture with initial values specified as dry over desert regions, rain in the early stages of the experiments moistened the southern region of the Sahara and the rain area gradually extended northwards over the first 20 days. Clearly, starting from a drier Saharan atmosphere might prevent this unrealistic behaviour. Another factor which may be important is the radiation scheme, as illustrated by experiments carried out with a 5-layer model (Slingo 1979). Starting from realistic initial conditions, Slingo found a marked improvement in the July rainfall distribution over the Sahara when an 'interactive' radiation scheme, with cooling rates dependent on modelled water vapour though with fixed, zonally-averaged, climatological clouds, was used in place of a simpler 'climatological' one. A likely explanation for this is the higher infrared surface cooling and reduced atmospheric cooling noted by Slingo during the first few days with the interactive scheme, which result in less sensible heat flux from the surface and less convective activity than with the climatological scheme. This can be attributed to the effects of water vapour whereby with dry Saharan air less downward infrared flux reaches the surface than with a moist atmosphere; the climatological scheme makes no allowance for this.

In this paper a series of experiments are described which show the sensitivity of the Saharan region to atmospheric moisture, soil moisture, the radiation scheme used and finally the surface albedo.

2. Model and initial conditions

The 11-layer, global primitive equation model is a high resolution version of the Meteorological Office 5-layer model described by Corby et al (1977). The horizontal grid consists of rows of points every 2^{o} of latitude (222 km) with east-west spacing also of about 222km. The vertical coordinate is sigma (pressure divided by its surface value); its values at the boundaries and mid-points of each of the 11 layers are given in Table 1. The basic dynamical equations and finite difference approximations are given in Corby et al (1977). The model uses a leapfrog integration scheme with time smoothing and non-linear horizontal diffusion (Saker 1975). Changes to the finite difference scheme were needed to maintain energy conservation with uneven vertical resolution; these are described in the Appendix.

Physical processes include the treatment of an interactive surface. Soil moisture content (SMC) is increased by rainfall and melting snow except that any excess over 15cm is assumed to run off; it is decreased by evaporation at the potential rate, E_p, for SMC $\geqslant$ 5cm but at a reduced rate (E_p x SMC/5cm) for SMC $<$ 5cm. The weakness of this formulation is discussed by Rowntree (1982): a rapid increase of modelled E_p, which is proportional to the difference between the saturated specific humidity at the surface temperature and the atmospheric specific humidity, occurs as the surface temperature increases when the soil is drying out; this results in a slower decrease in evaporation than the linear relation suggested by the formula and by observations (Priestley and Taylor, 1972) until the soil moisture content is well below 5cm. Precipitation falls as snow until it reaches a layer with temperature above 273K where it is melted, taking the necessary heat from that layer. Snow depth is incremented by snowfall reaching the ground and decreased by melting and sublimation. Surface albedos are taken as 0.2 for all snow-free land, 0.5 for snow-covered land, 0.8 for both sea ice and land ice and 0.06 for sea. The effective heat capacity of the land surface is taken as 20.9 J $cm^{-2}K^{-1}$, this value being chosen to represent diurnal

variations for a typical soil.

The treatment of the boundary layer is based on Method 1 of Clarke (1970); the boundary layer is assumed to occupy the three lowest model layers and transfers of heat, moisture and momentum between the layers are modelled by an eddy diffusivity approach (Carson 1982). The convection scheme, described by Lyne and Rowntree (1976), is designed to represent the effects of deep penetrative convection. It is based on the concept of an ensemble of buoyant plumes of varying characteristics, starting at one level and extending upwards to different heights dependent on their properties. The ensemble grows by entrainment until it reaches a layer in which it is no longer buoyant. Its buoyancy is then maintained by detrainment of the less buoyant plumes until it becomes smaller than a critical size or reaches the maximum height achievable by an undilute parcel. Both moist and dry convection are modelled, as is the ice phase and the evaporation of condensates. Large-scale precipitation occurs to remove super-saturation as in Corby et al (1977).

The model is used here with two different radiation schemes. The earlier one is a simple, climatological scheme based on that for the Meteorological Office 5-layer model given in Corby et al (1977). To achieve greater realism and flexibility, Walker (1977) developed an interactive radiation scheme which assumes fixed, zonally-averaged, climatological clouds; the scheme is similar to that for the 5-layer model which she described in Slingo (1982). The crucial difference between the two schemes relevant to this work is the interaction between water vapour and radiation present in the interactive but not in the climatological scheme in which long wave cooling depends only on temperature, latitude, pressure and season, whilst solar heating is prescribed.

In all the experiments, the radiative conditions and fixed sea surface temperatures are those appropriate to July. The initial atmospheric conditions were either the same as in the earlier experiments which produced excessive rainfall over the Sahara or were modified by using lower values of specific

humidity over North Africa. This was done over the area 10° - 32°N, 15°W - 35°E by inserting one value at each model level. These values were means for the area based upon data for 27 May 1977 and are in good agreement with climatological estimates over the Saharan region in July (Newell et al, 1972). Fig. 1 shows the area where changes were made and Table 1 lists the initial specific humidities (q) meaned over this area for the moist and dry atmospheres. The negative values at the top two levels in the moist case result from vertical extrapolation from data for a different model; they are not used by the radiation scheme which assumes the minimum of the modelled value and 1.0×10^{-4} g kg^{-1}. The initial soil moistures are specified as zero over deserts and 10 cm elsewhere; the boundaries of the dry region over North Africa are shown in fig. 1. Table 2 lists the different combinations of radiation scheme and initial conditions used in the experiments. In two experiments changes were made to the soil moisture content over the area 10° - 32°N, 15°W - 35°E; one experiment (I3) started with moist soil (SMC = 10 cm) and in the other (I4) the soil was kept dry (no evaporation allowed) throughout the integration. The last experiment, C2a, was designed to assess the effect of varying the surface albedo in a realistic way over Africa; it was fixed at 0.2 over all snow-free land surfaces in the other six experiments.

3. Results

(a) Effect of the initial atmospheric moisture

Rainfall

The importance of initial atmospheric moisture is shown by comparing the two 50-day experiments I1 and I2 which started from moist and realistically dry Saharan atmospheres respectively and used interactive radiation. Fig. 2 gives their day 21-50 mean rainfall amounts which, whilst differing considerably over North Africa and also over the Atlantic at 10°-15°N, are generally similar outside the area shown. In I1, sporadic

outbreaks of rain occurred over the Sahara in the first few days, then heavier rain spread northwards at 0° - 20°E around day 10. Thereafter rainfall generally increased over North Africa with the maximum of the main rainfall belt becoming established at 15°N, although the region east of 20°E at 20° - 30°N remained dry. In I2, rainfall up to day 7 was limited to south of 10°N with the main rainbelt maximum at 7°N. After that, small amounts of rain occurred north of the rainbelt which itself moved north to be centred at 11°N by day 20. Thence to day 50 conditions changed little with the rain belt occupying 5° - 20°N. The position and intensity of the maximum rainfall, and the northward extent of the rain belt are near to the observed (Jaeger, 1976) which has its maximum at 9°N, although the modelled southern limit of the rainfall is about 7° too far north.

Fig 3 shows that the daily rainfall meaned over the Saharan region, whilst displaying marked fluctuations, increased generally throughout experiment I1 to reach near 4 mm day^{-1} by day 50 with a corresponding moistening of the soil, whereas in I2 it never exceeded 0.8 mm day^{-1} and the soil moisture content remained close to zero. The atmospheric water content in I1, although decreasing up to day 8, then increased and always remained well above the values in I2 with the difference between the two experiments at day 50 similar to that at the initial time.

Interaction of radiation and circulation

The increase in total (soil + atmosphere) moisture content in I1 indicates the existence of a net inflow of water vapour into the Saharan region, which implies a different circulation to that obtained in I2. To understand this, it is instructive to consider the radiative quantities shown in Table 3. In I1 the greater water vapour content increases the infra-red opacity in the water vapour absorption bands and therefore also the downward infra-red flux compared to that in I2. The effect of this on net surface

radiation is shown in Table 3 by the sum of sensible and latent heat flux which is equal to the net surface radiation except for a very small contribution due to the heat flux into the ground. This leads to enhanced convective activity and, with the additional effect of a lower condensation level in I1, more rain. The net radiation at the top of the atmosphere is also greater, with day 16 values averaged over the Saharan region (Table 3) of 63.7 Wm^{-2} in I1 compared to 48.3 Wm^{-2} in I2.

The increase in rainfall implies there is more ascent; this is confirmed later in Fig.12. This coincidence of an increase in ascent with an increase in net radiation at the top of the atmosphere is consistent with Charney's hypothesis (see section 1) in that the greater net radiation requires more ascent, with energy export at high levels, in I1 to achieve an energy balance. However it is likely that the major contribution to the changes is the difference in moisture distributions. This is evident from the experiments of Walker and Rowntree (1977) with an idealised version of Northern Africa extending from 6^{o} to $32^{o}N$ in a limited-area model. They ran two experiments, one with all the land initially moist, the other with all but 6^{o} to $14^{o}N$ initially arid. In the 'wet' experiment they obtained more widespread and intense rainfall, the mean meridional circulation consisting of a deep cell in the meridional plane, while the 'dry' experiment gave less rainfall confined over the wet land and a meridional circulation dominated by a shallow dry vertical circulation. This contrast cannot be attributed to the Charney mechanism because the radiative heating rates were prescribed at the same values in each experiment. It thus appears that the atmospheric moisture distribution can directly modify the vertical circulation. This may be regarded as an extension of Charney's hypothesis to allow for moisture so that where there is diabatic heating (eg by latent heat release) there must be advective cooling which in the tropics is likely to be by ascent of potentially cooler air. Where the air is dry as over the Sahara the upper troposphere has diabatic (radiative) cooling while the lower layers are heated by turbulent and convective heat transfer from the surface. Thus shallow ascent in the lower

troposphere is to be expected with descent in the upper troposphere, a similar type of circulation to that obtained in Charney's simple model. If the Saharan troposphere becomes moist, either through advection or evaporation from the surface, latent heating can occur in the middle and upper troposphere leading to a breakdown of the circulation developed in the absence of moisture.

Temperature

Most of the net surface radiation is used for sensible heat flux in I2 giving vigorous but shallow dry convection, whereas in I1, once the surface has moistened, it is used mainly for evaporation with subsequent latent heat release in deep convection. This is reflected in the temperature differences (Fig.4) in that I2 is warmer below 600 mb particularly near 20°N and cooler from 600 mb to 250 mb than I1. Note that this is for midnight; results using data at 6 hour intervals are very similar. This pattern resembles that obtained by Walker and Rowntree (1977) (their Fig.2), in which changing from a moist to a dry surface gave temperature decreases at 500 mb to 200 mb with increases elsewhere, as the structure forced by moist convection was replaced by one close to the dry adiabatic from the heated surface up to mid-troposphere, with radiative cooling and subsidence above.

Lower tropospheric circulation

The temperature differences are sufficient to cause a markedly different circulation at 700 mb (Fig.5) with easterlies over North Africa at 10°-20°N in I2 in contrast to westerlies at 5°-15°N in I1. The circulation in the Atlantic is also altered with the area centred near 10°-15°N, 30°-60°W receiving more rainfall in I2 (Fig 2), in easterlies coming directly from Africa, than in I1 where the 700 mb flow has originated from further north in the Atlantic sub-tropical high pressure region. Fig 6 shows the westerly (u) and southerly (v) wind components

meaned across the longitude band 10°W - 30°E and also gives the corresponding cross sections at 20°E taken from Newell et al (1972). For the zonal component I2 agrees much better with the observed than I1 where the westerlies at 10° - 20°N occupy too deep a layer up to near 500 mb. Newell and Kidson (1984) have reported a difference in the same sense in 850 mb August zonal winds at 15°N from 15°W to 15°E between a relatively wet period (1958-1962) and a dry period (1970-1973) in the Sahel with easterlies weaker by 1.5 to 3.5 ms^{-1} in the wetter Augusts.

Dennett et al (1985), following up the earlier study by Bunting et al (1975), found that 700 mb height at Niamey (13½°N, 2°E) is higher in drier Augusts than normal Augusts, the difference associated with an anomaly of 40% from the normal being about 40gpm. In the model, 700 mb heights are greater in I2 than I1 over the region of decreased rainfall with a maximum difference in the day 21-50 mean of about 40gpm near 20°N, 0°E. The cause of the modelled difference, warming of the lower troposphere, probably also contributes in the real case, though the size of the observed difference relative to the perturbation appears larger than for the model.

The results shown so far are based upon data averaged for midnight; to assess any bias this might produce, the last ten days of I1 and I2 were repeated storing the results every six hours. Ten-day means were then produced for 0000, 0600, 1200 and 1800 GMT and for an average of these times. At midnight the results are broadly similar to those for the day 21-50 mean. There is little diurnal variation in the westerly wind components, but some changes in the meridional flow (Fig. 7). McGarry and Reed (1978) studied the observed diurnal variation of winds at 600 to 900m during summer 1974. They found evidence of wind fluctuations of 1-3 ms^{-1}; at 00 GMT, deviations from the 24 hour mean were mostly towards north to northeast and at 12 GMT towards south to southwest at 10°W - 10°E, 5° - 17°N. These variations are of similar sense and size to those shown at this level in Fig. 7. The writers know of no evidence concerning such variations at higher levels, though a return flow would be expected at some upper level.

In I1 the region of southerlies at 20° - 30°N, 700-800 mb, present at midnight, reverses at midday and is barely evident in the overall mean; it is not present in I2. Figure 8 shows the differences between I2 and I1 for the day 21-50 mean at midnight only; at days 41-50 the overall mean differences are similar apart from having a weaker peak near 23°N above 300 mb. The meridional winds differ mainly north of 15°N, I2 having more southward flow below about 500 mb and less above. Both these changes are towards the 20°E climatology though it should be noted that Newell et al's maps indicate that the 10°W - 30°E mean would have weaker peaks near 700 mb and 150 mb at 30° - 35°N, whilst the southerly near 700 mb and 20°N would be even weaker. Newell and Kidson (1984) found increased northerlies through much of the troposphere in their 'dry August' composite from about 10° to 20°N. The more northerly location of this feature in the model could be consistent with the fact that the perturbation of the forcing here affects much of the Sahara as well as the Sahel.

Upper tropospheric circulation.

Figure 6 also shows a weaker easterly flow in the upper troposphere in I2. Figure 9 shows that these differences cover a large area of Africa and the tropical Atlantic. North of the equator these changes are consistent with the cooling of the upper troposphere and associated decreased geopotentials over North Africa. Vector wind differences (not shown) approximately mirror those at 700mb with a cyclonic circulation in I2 relative to I1 centred near 25°N,0°E. The year-to-year variability of this version of the model is not known, but for an 8 year integration with a version of this model similar apart from having a poorer ($2\frac{1}{2}^{\circ}$ x $3^{3}/4^{\circ}$) horizontal resolution, the standard deviation (7 degrees of freedom) of u at 250 mb for July is less than 2 ms^{-1} over most of Africa north of the equator and about 4 ms^{-1} over the equatorial Atlantic. The westward extension of the increased westerlies to the east Pacific and the decreased

westerlies near Indonesia may be chance variations, the physical mechanism being unclear, though the changes are more than twice the local standard deviation ($\sim$ 2 ms^{-1}). Similar remarks apply to the changes of 10 ms^{-1} south of the equator over Africa and the Atlantic where standard deviations in the 8 year run were over 4 ms^{-1} with a maximum of 7 ms^{-1} over central southern Africa. Weakening of the 200 mb easterlies was obtained in integrations with increased Saharan albedo by Laval (1983). This is consistent with our experiments as in both cases the North African heat source is weakened.

There is also, as noted by Laval, observational evidence that the upper easterlies tend to be weaker in drought years. Kidson (1977) found a correlation coefficient of 0.79 between rainfall at 15°N from 5°W to 30°E and 200 mb wind speeds from 0° to 15°N at 10°E for Augusts of 1958-62 and 1970-73. During the dry Augusts of 1972 and 1973 the wind speed (presumably the westward component) was 5 to 10 ms^{-1} less than in the other Augusts. Newell and Kidson (1984)'s maps of differences at 200mb show increased eastward components for their dry August composite over most of tropical Africa with largest increases near 5° - 10°N and 20°S. Fig. 9(b) shows some similarity to this but lacks an observed maximum change near 10°N 45°E, and has changes near 20°N not evident in the observed. Again, in view of the different characteristics of the model and observed perturbations, the results are perhaps as similar as could be expected. Kanamitsu and Krishnamurti (1978) compared the 200 mb flow regime of June to August of 1972 to that of 1967 (a 'normal' year) and found similar anomalies over tropical Africa and the tropical Atlantic. However, as they point out, the tropical east Pacific was very warm during summer 1972, and subsequent numerical model experiments (Keshavamurty (1982), Rowntree (1978)) have shown that such an anomaly tends to weaken the upper easterlies over most of the equatorial belt except near the anomaly. There is no clear evidence for a relation between Sahel rainfall and equatorial east Pacific sea surface temperatures (Kidson 1977, p. 454).

Moisture flux and vertical motion

The net inflow of water vapour into the Saharan region in I1 is probably caused by the northward moisture flux (the time-mean of vq, shown in Figs.10 and 11) associated with the southerlies south of 20°N below 850 mb and through a greater depth at 20° - 25°N. In I2 there is vertically integrated poleward flux only south of 12°N, the flux being greater in I1 at all latitudes from the equator to 30°N. More of the northerly return flow (Fig. 7) occurs at a lower height in I2 than in I1 particularly at 15° - 20°N; as discussed earlier, this is similar to results obtained by Walker and Rowntree (1977) (their Fig. 4) when changing from a dry to a moist soil. In I2 at 10° - 20°N there are southerlies below 800 mb at midnight, whereas at midday these are restricted to a much shallower layer. These differences are associated with variations in 500 mb vertical velocity (Fig. 12), which in I2 are particularly pronounced with strong ascent near 11°N at midday (over the rain belt) and weaker ascent near 19°N at midnight. Diurnal variations of low level convergence are evident in the analysis of observed winds by McGarry and Payne (1978) already referred to and are implied by the rainfall data of Burpee (1977) analysed by McGarry and Payne. In both experiments the overall mean ascent is well correlated to the rainfall (for which the day 41-50 mean is similar to the day21-50 mean); note particularly the contrast between the experiments at 20° - 30°N with general ascent in I1 and descent in I2. The ascent is associated with convergence near 750 mb and divergence near 250 mb, mainly from the meridional winds (cf Figs 7(c) and (f)) but with some contribution from the zonal winds in I1.

Summary

These results show that in the dry case the moist low-level south-westerly winds flowing towards the Sahara do not provide northward moisture flux beyond about 12°N whereas in the moist case there is more poleward flux so providing a net inflow of moisture into the Saharan atmosphere. Although both experiments have a surface Saharan low pressure region (not shown but evident from the zonal winds in Fig. 6), the warm air at low levels in

I2 transforms this into a high at 700 mb, whereas with the cooler air in I1 there is a deeper cyclonic circulation with a 700 mb centre at 20°N, 0°E, as indicated by the flow patterns in Fig. 5. There are associated major changes in the upper tropospheric circulation, vertical motions and rainfall distribution.

(b) Effect of the soil moisture

In the experiment with the initial realistically dry atmosphere but moist soil over the Saharan region, I3, the atmosphere quickly moistened as shown in Fig. 3(c) so that by day 4 it was as moist as in experiment I1 which started from the moist atmosphere and dry soil. This was due to evaporation rates slightly over 5 mm day^{-1}, which, accompanied by only small amounts of rain at first, provided a large moisture flux into the atmosphere. In response to this, rainfall over the Saharan region (Fig. 3(b)) increased rapidly, exceeding that in I1 near day 4 before levelling off after day 11. The soil in I3 provided a large reservoir of moisture since the initial content of 10 cm is considerably more than the 1.7 cm difference between the equivalent amounts of water present in the initial atmospheres. This fact together with the potentially large evaporation rates in these regions make it not surprising that excessive rainfall soon developed in the Sahara with the moist initial soil, as shown for the day 7-16 mean in Fig 13. Rainfall exceeds 2mm/day over much of North Africa with some areas of over 5 mm/day north to 25°N and at 30° - 35°N. There are similar changes in the 700 mb flow to those shown in Fig. 5 (see Rowntree 1983).

The change in net surface radiation relative to experiment I2, shown approximately in Table 3 by the sum of sensible and latent heat for days 7-16, is very large. This must again be due to longwave radiation, as moistening of the atmosphere tends to slightly reduce the net downward solar radiation. As cloudiness is prescribed, the reduction in the upward flux associated with the cooling of the surface by 10.6 K outweighs the reduction in the downward component; this contrasts with the usually small dependence of net

surface longwave radiation on temperature. For a surface cooling of 10.6 K the upward flux decreases by about 61 Wm^{-2} so that even with no reduction in solar flux, the decrease in downward flux would be only 6.5 Wm^{-2}; this is probably a lower bound since the surface temperature difference is likely to be relatively small at midnight; data for other times are not available from I2 and I3 at days 7-16 but data for I2 and I1 at days 41-50 show a surface temperature difference of 5.3 K for the mean of 00, 06, 12 and 18 GMT compared with 4.15 K at 00 GMT. That the decrease in downward flux is so small despite the large cooling of the lower troposphere is clearly due to an increase in atmospheric moisture content (Table 4); this moistening is particularly marked near the ground, specific humidity increasing from 6.3 to 13.0 g/kg.

In the experiment, I4, starting from the moist atmosphere over the Saharan region but with the soil kept dry throughout the integration, the atmosphere dried out (see Fig. 3) through rain falling but not being allowed to evaporate from the surface. Inflow of moist air was insufficient to balance this and by day 18 its atmosphere was drier than in experiment I2. Rainfall over the Saharan region averaged 1 mm day^{-1} for the first 10 days and then declined to reach values similar to those in I2 by day 19. This further emphasizes the importance of evaporation in such regions where evaporation rates are potentially high; probably one reason why desert regions are dry is the low water capacity of unvegetated surfaces. This allows rain to drain away quickly from the shallow surface layer from which evaporation is possible whereas over vegetated surfaces the roots are able to bring water up from a much deeper layer.

(c) Effect of the radiation scheme

The importance of the radiation scheme used is shown by comparing the pair of experiments I1 and I2 with the corresponding pair C1 and C2 which started from identical conditions but used the climatological radiation scheme. Rainfall over the Saharan region (Fig. 3) is consistently

greater over the first 10 days with climatological radiation despite similar atmospheric water contents. To understand this it is necessary to consider how the climatological scheme works. It uses zonally-averaged climatological clouds, implicitly rather than explicitly as in the interactive scheme. This means that over regions with less cloud than the zonal average such as the Sahara the solar heating, being a specified zonal average, is underestimated at the surface by a similar amount in both schemes. The important difference arises from the lack of interaction with water vapour in the climatological scheme where specified zonally averaged longwave cooling coefficients are used solely in conjunction with model temperatures to give longwave cooling rates. As the cooling coefficients are derived from radiative calculations by Rodgers (1967) with a zonally averaged climatological atmosphere, the implied humidity profile is too moist for the Sahara leading to unrealistically large net surface heating there; this leads to enhanced convection and more rainfall relative to the interactive case. The consequent change in the mass fields then modifies the circulation allowing advection of moist air northwards into the Sahara and displacing the drier air initially present in experiment C2. This is seen in Fig. 3(c) where, after day 10, C2 increasingly has a moister atmosphere than I2. After day 20 C1 has a drier atmosphere than I1; this may be due to the model's variability since another experiment using climatological radiation but starting from different initial data gave an atmosphere about as moist as in I1. Means taken over the Saharan region for days 7-16 (Table 3) show greater soil moisture content, rainfall, evaporation and sensible heat flux with climatological radiation for both the moist and realistically dry initial Saharan atmospheres. The net downward radiation at the top of the atmosphere is also greater in C2 than I2, with respective values averaged over the Saharan region of 56.2 Wm^{-2} and 48.3 Wm^{-2} for day 16, so encouraging more ascent when the climatological scheme is used than with the interactive one as discussed in Section 1. Thus the greater net radiation calculated

with the climatological scheme, with a realistically dry initial Saharan atmosphere, appears sufficient eventually to produce excessive rainfall in the Sahara.

(d) Effect of the albedo

This is shown by comparing experiment C2, the climatological radiation experiment starting with the dry soil and the realistically dry Saharan atmosphere, with experiment C2a which differs only in that the albedo over Africa and Arabia was changed from the fixed value of 0.2 used in the other experiments. The albedo distribution (H.P. Walker, unpublished Met O 20 note) used a subdivision of Africa into land-use areas based upon those in the New Oxford Atlas. A mean albedo value derived from measurements taken from several different sources was allocated to each of the land-use types. Fig 14 shows the albedo distribution so obtained which has values ranging from 0.14 for equatorial forest to 0.28 for desert. This latter figure is lower than the 0.35 used by Charney et al who took their values from only one source, that documented by Rockwood and Cox (1978). The actual albedos for deserts depend strongly on the nature of the surface (sand colour, etc). Note that our tropical forest albedos are well above the 0.07 proposed by Posey and Clapp (1964) which is based on observations in the visible ($< 0.7\ \mu m$) part of the spectrum (Rowntree 1975, Dickinson 1980).

Daily rainfall amounts, zonally meaned over days 7-16 for Africa and Arabia (Fig. 15) are shown in Fig. 16 to decrease where the albedo has been raised and increase where it has been lowered except for the small area south of $28^{\circ}S$. The maximum at $11^{\circ}N$ of 7.4 mm day^{-1} for the fixed albedo of 0.2 has moved southwards to $9^{\circ}N$ in the variable albedo case where it has intensified to 8.8 mm day^{-1} with the lower albedo. The geographical distribution of the rainfall differences produced by the change in albedos (Fig. 17), whilst reflecting the changes in the zonal means, shows the patchy nature of convective rainfall particularly over the Saharan region where increases do occur despite the general decrease. Such patchiness will tend to decrease as the sampling period increases. The changes are

largest in an 8° wide latitude belt centred at 10°N from 15°W to 30°E where model rainfall averages 5-10 mm day^{-1} and the albedo has been decreased to 0.14 in the southern half and increased to 0.24 in the northern half. In this belt average rainfall increases by 2.4 mm day^{-1} where the albedo has been lowered and decreases by 2.4 mm day^{-1} where the albedo has been raised.

These rainfall changes are generally in phase with changes noted in the evaporation (not shown) which south of the equator show a close correspondence to the albedo distribution with decreased evaporation over the area with albedo of 0.28 surrounded by increases. This is reasonable since an increase in albedo will cause a decrease in the net downward radiation at the top of the atmosphere, so encouraging descent and reduced rainfall as discussed in Section 1. In addition the surface net radiation is less leading to a decrease in the energy available for evaporation; this can also be expected to decrease the rainfall as discussed in Section 3(c). Over the Saharan region where the albedo has been raised from 0.20 to 0.28, Table 3 shows these changes with a decrease in daily rainfall, meaned over days 7-16, from 1.09 to 0.84 mm day^{-1}. Fig. 3 shows that the rainfall decrease was general throughout the 20 days of integration; moreover the atmospheric water content shows noticable decreases towards the end of the period. Similar dependences of modelled rainfall on albedo have been found both for small areas (Charney et al 1977, Sud and Fennessy 1982) and large areas (Chervin 1979, Henderson-Sellers and Gornitz 1984, Carson and Sangster 1981) as reviewed by Rowntree (1984).

This experiment can be most directly compared with a similar one carried out by Charney et al in which increasing the albedo from 0.14 to 0.35 over the Saharan and Arabian deserts produced a decrease in modelled July mean rainfall over these regions from 4.21 to 2.63 mm day^{-1}. Their rainfall rates were high probably because the formulation of ground hydrology resulted in too much evaporation over land.

4. DISCUSSION AND CONCLUSIONS

The experiments reported here clearly show that the Sahara can be a sensitive region in general circulation models as measured by changes in rainfall and circulation. Given a moisture dependent radiation scheme and a moist atmosphere, either introduced initially or produced by rapid evaporation from a moist surface, the radiative energy input is greater than with a drier atmosphere; this favours enhanced mean ascent and convective activity. There is a cyclonic circulation in the middle troposphere which causes inflow of moist air and excessive rainfall over the Sahara. However with a typically dry desert atmosphere, net downward radiation is less and inflow of moist air is weakened; there is an anticyclonic circulation in the middle troposphere and descending motion above, so keeping the region dry. Thus the simulation of a dry Sahara in the model used here requires the combination of a realistically dry initial atmosphere, an initially dry soil and the use of a radiation scheme which takes account of variations in atmospheric humidity. In addition the rainfall distribution over Africa has been shown to be sensitive to changes in albedo with increased and decreased albedos generally giving rainfall decreases and increases respectively.

The results presented here may be relevant to the existence of much moister conditions over the Sahara during the early Holocene (around 9000 yr B.P.) (Street and Grove, 1979). It appears that, with a surface moisture source, from, for example, deep-rooting deciduous vegetation, a summer rainy season could exist as in some other areas at this latitude of both hemispheres. Kutzbach and Otto-Bliesner (1982) have suggested that the increased summer solar radiation around 9000 yr B.P. was at least partly responsible for the different African climate of that time. A combination of these two mechanisms may provide the solution to this problem.

The importance of vegetation in this context deserves more discussion. In a subtropical climate with a long dry winter, perennial woody vegetation

can provide access in summer to the soil water through a much greater depth than is possible with bare soil, whilst conserving this water, by loss of foliage, during the dry season. Rutherford (1984) describes the seasonal cycle of woody vegetation at 24°S in the Transvaal. The spring growth of new foliage occurs in response to light and warmth before the rainy season starts, using either soil moisture near the roots or water stored in the plant. Thus evapotranspiration is small or zero in the dry season but restarts in early summer using water from the previous wet season and, as soon as it is available, from the first summer rains.

Conversely, the results from the model show that rainfall may be prevented by absence of soil water storage as in experiment I4. This is a similar result to those of Shukla and Mintz (1982) and Sud and Arakawa (reported by Mintz (1984)) though in those experiments the suppression of evaporation was on a global scale. Although total inhibition of evaporation is not possible, the condition may be approached with bare soils such as may be produced through overgrazing in the Sahel region (Mensching 1980). The lack of vegetation prevents interception (and subsequent evaporation) of the rainfall, so reducing the rapid short-term feedback of moisture to the atmosphere which is important in the moist tropics (Shuttleworth et al, 1984). With no roots, much of the water that does infiltrate into the soil can pass too deep for subsequent diffusion to the surface, either raising the water table or leaving a deep moist layer of soil or sand which can persist for years (Cloudsley-Thompson, 1977, p. 12). Where crusting of the surface occurs due to drying out after rain, a larger part of the next rainfall runs off (Mensching 1980). Except when dormant vegetation can take advantage of the occasional heavy rainfall (e.g. through seed germination), moisture will only be readily available for evaporation for the day or two after rain before the surface dries. In the Sahel, rainfall is modulated by easterly waves which have a period of about four days (Burpee 1974, Reed 1978). This period is long enough for the surface soil layer to dry out, so that, in the absence of vegetation to tap the deeper soil, surface evaporation may provide little

of the moisture needed for rain (see also Mensching 1980, Perrier 1982, p. 402, Warren and Maizels 1977).

This theory is consistent with the analysis of recent Sahel rainfall by Dennett et al (1985) which shows that the decrease in rainfall is small in June and a maximum in August and September, suggesting that the onset of the rains, presumably due to moist advection from the south, is normal and that it is the contribution of local evaporation to the maintenance of the rainfall which is deficient.

In the context of past Saharan climates, the significant result here is thus that a supply of moisture for evaporation in summer may be sufficient to maintain a summer rainfall regime over much of the Sahara. The conservation of deep water with deciduous vegetation allows the annual soil water budget to be essentially that for the summer. In the model used in our experiments, as shown by the moisture budget for experiment I1 in Fig. 3, this summer water budget can be such that moisture is still being supplied to the region even after the soil has become quite moist. This interpretation, is not intended to be an explanation of the moister climate believed to have affected the Sahara, merely a contribution to the understanding of how a moister climate once established could have been maintained.

Surface albedo has been shown here to provide feedbacks in the same sense as soil moisture, rainfall increasing as the albedo decreases. Such a chance may be achieved in nature by moistening of the soil or by growth of vegetation. Though its role appears to be secondary from these experiments, giving relatively minor changes of rainfall compared to those associated with the moisture changes, it could perhaps in some circumstances be critical, the interaction of albedo and the moistness of the surface, not considered here, maybe of particular importance, as discussed by Rowntree (1983).

There are three limitations in the model in its present form which affect its simulation over North Africa. Firstly, the use of fixed zonally-averaged climatological cloud amounts, used in the radiation calculations only,

introduces too much cloud into the desert region. This decreases the absorbed solar radiation by increasing the planetary albedo, but also decreases the outgoing infra-red radiation by absorbing that from the surface and emitting at a lower temperature. This would produce a net change in temperature, the sign of which is uncertain (Cess et al, 1982). It appears more likely that an increase of cloud in the desert region produces a cooling; if so the difference between the experiments which gave a wet or a dry Sahara will have been exaggerated. This deficincy could be investigated by introducing a longitudinal variation into the prescribed clouds or by the use of an interactive cloud scheme. Secondly, the use of a constant snow-free land surface albedo, as indicated by the experiment with a varying albedo, may result in too much rainfall over deserts and too little over low albedo regions such as forests. Albedo also depends upon the soil moisture, in such a way that moistening the surface decreases the albedo, both for vegetation and bare soil, as in Norton et al (1979) and Idso et al (1975). This lower albedo may again give rise to increased rainfall as discussed by Rowntree (1982), so providing a positive feedback effect. Finally, the treatment of hydrological processes may be important in that over deserts rain drains away quickly from the surface layer easily accessible to evaporation whereas over forests a much larger proportion of the rainfall is available for evaporation. The model in its present form treats all land surfaces alike. A more realistic treatment of land surface hydrology with geographically varying soil and vegetation characteristics is needed for proper representation of these effects.

Appendix. To maintain energy conservation with uneven vertical resolution, the finite difference forms of the hydrostatic relation and of the $\kappa\omega T/\sigma$ term have been modified from the forms given in Corby et al (1977). Thus their equation(7) is replaced by

$$\phi_k = \phi_* + \sum_{s=k+1}^{n} \left[RT_s \ln\left(\sigma_{s+\frac{1}{2}} / \sigma_{s-\frac{1}{2}}\right)\right] + C_k R T_k \ln\left(\sigma_{k+\frac{1}{2}} / \sigma_{k-\frac{1}{2}}\right)$$

and the first line of their equation (13) is replaced by

$$\left(\kappa T_k / \sigma_k\right)\left[\sum_{s=1}^{k-1} (\nabla . \underline{V}_s)\sigma_s \ln\left(\sigma_{s+\frac{1}{2}} / \sigma_{s-\frac{1}{2}}\right) + C_k (\nabla . \underline{V}_k)\sigma_k \ln\left(\sigma_{k+\frac{1}{2}} / \sigma_{k-\frac{1}{2}}\right)\right]$$

where $(\nabla . \underline{V}_s) = (1/a\cos\theta)(\delta_\lambda U_s^{-\lambda} + \delta_\theta V_s^{-\theta}\cos\theta)$

and similarly for $(\nabla . \underline{V}_k)$ (other notation as Corby et al (1977)).

The interpolation constants C_k in these two expressions must be equal for energy conservation but are otherwise arbitrary. They are defined as $\ln(\sigma_{k+\frac{1}{2}}/\sigma_k) / \ln(\sigma_{k+\frac{1}{2}}/\sigma_{k-\frac{1}{2}})$. It is also necessary to define the σ_k by

$$\sigma_k \Delta(\ln\sigma)_k = \Delta\sigma_k$$

where $\Delta(\ )_k \equiv (\ )_{k+\frac{1}{2}} - (\ )_{k-\frac{1}{2}}$.

Note that in the top layer $(k=1)$ $\Delta(\ln\sigma)_k$ is ill-defined as $\sigma_{\frac{1}{2}} = 0$. σ_1 is specified as $e^{-1}\sigma_{1\frac{1}{2}}$ and $\Delta(\ln\sigma)_1$ follows from the relation

$$\sum_{k=1}^{n} \Delta\sigma_k = \sum_{k=1}^{n} \sigma_k \Delta(\ln\sigma)_k = 1$$

The last condition for energy conservation is that when interpolating for u and v at layer boundaries (for $\bar{u}^\sigma, \bar{v}^\sigma$) it is necessary to give equal weights to the u and v in the layers above and below. For temperature T and specific humidity q, this constraint does not apply and the weights were designed to give correct boundary values for T when the lapse rate is dry adiabatic and for q with a typical logarithmic lapse rate. A more detailed discussion of the energy conservation properties of the model is given by Saker (1975).

REFERENCES

Bunting, A.H., Dennett, M.D., Elston, J. and Milford, J.R. 1975 Seasonal rainfall forecasting in West Africa. Nature, 253, 622-623.

Burpee, R.W. 1974 Characteristics of North African easterly waves during the summers of 1968 and 1969. J. Atmos. Sci., 31, 1556-1570.

Burpee, R.W. 1977 The influence of easterly waves on the patterns of precipitation in tropical North Africa. WMO No. 492, 40-71.

Carson, D.J. 1982 Current parametrizations of land surface processes in atmospheric general circulation models. In 'Land-surface processes in atmospheric general circulation models'. Ed. P.S. Eagleson. Cambridge University Press, pp 67-108.

Carson, D.J., and Sangster, A.B. 1981 The influence of land surface albedo and soil moisture on general circulation model simulations. Numerical Experimentation Programme Report No. 2, pp 5.14-5.21.

Cess, R.D., Briegleb, M.S., Lian, M.S. 1982 Low latitude cloudiness and climate feedback: comparative estimates from satellite data. J. Atmos. Sci., 39, pp 53-59.

Charney, J.G. 1975 Dynamics of deserts and drought in the Sahel. Quart. J.R. Met. Soc., 101, pp 193-202.

Charney, J.G., Quirk, W.J., Chow, S. and Kornfield, J. 1977 A comparative study of the effects of albedo change on drought in semi-arid regions. J. Atmos. Sci., 34, pp 1366-1385.

Chervin, R.M. 1979 Response of the NCAR general circulation model to changed land surface albedo. GARP report of the JOC study conference on climate model. Vol. 1, 563-581.

Clarke, R.H. 1970 Recommended methods for the treatment of the boundary layer in numerical models.

Austr. Met. Mag., 18, pp 51-93.

Cloudsley-Thompson, J.L. 1977 Man and the biology of arid zones. Edward Arnold (publ.). (182pp).

Corby, G.A., Gilchrist, A. and Rowntree, P.R. 1977 The UK Meteorological Office 5-layer general circulation model. Methods in Computational Physics, 17, pp 67-110.

Dennett, M.D., Elston, J. and Rodgers, J.A. 1985 A reappraisal of rainfall trends in the Sahel (submitted for publication).

Dickinson, R.E. 1980 Effects of tropical deforestation on climate. From 'Blowing in the wind: deforestation and long-range implications', No 14, Studies in Third World Societies, Dept Anthropology, College of William and Mary, Williamsburg, Va, pp 411-441.

Henderson-Sellers, A. and Gornitz, V. 1984 Possible climatic impacts of land cover transformations, with particular emphasis on tropical deforestation. Climatic change, 6, 231-257.

Idso, S.B., Jackson, R.D., Reginato, R.J., Kimball, B.A., and Nakayama, F.S. 1975 The dependence of bare soil albedo on soil water content.

J. Appl. Met., 14, pp 109-113.

Jaeger, L. 1976 Monthly maps of precipitation for the whole world.

Offenbach a.M., Wetterd., Ber. Bd. 18, Nr. 139.

Kanamitsu, M. and Krishnamurti, T.N. 1978 Northern Summer tropical circulations during drought and normal rainfall months.

Mon. Weath. Rev., 106, pp 331-347.

Keshavamurty, R.N. 1982 Response of the atmosphere to sea surface temperature anomalies over the equatorial Pacific and the teleconnections of the Southern Oscillation.

J. Atmos. Sci., 39, pp 1241-1259.

Kidson, J.W. 1977 African rainfall and its relation to the upper air circulation.

Quart. J. R. Met. Soc., 103, pp 441-456.

Kutzbach, J.E, and Otto-Bliesner, B.L. 1982 The sensitivity of the African-Asian monsoonal climate to orbital parameter changes for 9000 years B.P. in a low resolution general circulation model. J. Atmos. Sci., 39, 1177-1188.

Lamb, P.J. 1983 Sub-Saharan rainfall update for 1982; continued drought. J. Clim., 3, 419.

Laval, K. 1983 GCM experiments with surface albedo changes. Paper presented at Third International School of Climatology, Erice, Italy, October 1983.

Lyne, W.H., and Rowntree, P.R. 1976 Development of a convective parametrization using GATE data. Met O 20 Technical Note No. II/70, Meteorological Office, Bracknell.

McGarry, M.M. and Reed, R.J. 1978 Diurnal variations in convective activity and precipitation during Phases II and III of GATE. Mon. Weath. Rev., 106, 101-113.

Mensching, H.G. 1980 The Sahelian zone and the problems of desertification. Palaeoecology of Africa, 12, 257-266.

Newell, R.E. Kidson, J.W., Vincent, D.G., and Boer, G.J. 1972 The General Circulation of the Tropical Atmosphere and Interactions with Extratropical Latitudes. Vol. 1, MIT Press.

Newell, R.E., and Kidson, J.W. 1984 African mean wind changes between Sahelian wet and dry periods. J. Clim., 4, pp 27-33.

Nicholson, S.E. 1981 Rainfall and atmospheric circulation during drought periods and wetter years in West Africa. Mon. Weath. Rev., 109, 2191-2208.

Norton, C.C., Mosher, F.R. and Hinton, B. 1979 An investigation of surface albedo variations during the recent Sahel drought. J. Appl. Met., 18, pp. 1252-1262.

Perrier, A. 1982 Land surface processes:vegetation. In 'Land surface processes in atmospheric general circulation models' (ed. P.S. Eagleson), Cambridge University Press, pp. 395-448.

Posey, J.W. and Clapp, P.F. 1964 Global distribution of normal surface albedo. Geofisica Intl. 4, pp 33-48.

Mintz, Y 1984 The sensitivity of numerically simulated climates to land surface boundary conditions. pp 79-105 (chapter 6) of 'The Global Climate' (ed.J T Houghton). Cambridge University Press.

Priestley, C.H.B. and Taylor, R.J.	1972	On the assessment of surface heat flux and evaporation using large-scale parameters. Mon. Weath. Rev., 100, pp 81-92.
Reed, R.J.	1978	The structure and behaviour of easterly waves over West Africa and the Atlantic. Meteorology over the Tropical Oceans. Roy. Meteor. Soc., Bracknell, pp 57-71.
Rockwood, A.A., and Cox, S.K.	1978	Satellite inferred surface albedo over northwestern Africa. J. Atmos. Sci., 35, pp 513-522.
Rodgers, C.D.	1967	The radiative heat budget of the troposphere and lower stratosphere. Planetary Circulations Project Report No. A2, Dept. Meteorol., Massachusetts Institute of Technology, Cambridge.
Rowntree, P.R.	1975	The representation of radiation and surface heat exchange in a general circulation model. Met O 20 Technical Note No. II/58, Meteorological Office, Bracknell.
Rowntree, P.R.	1978	Statistical assessment of sea surface temperature anomaly experiments. Met O 20 Technical Note No. 11/132, Meteorological Office, Bracknell.
Rowntree, P.R.	1982	Numerical experiments relevant to the Sahel drought. Met O 20 Technical Note No. II/178, Meteorological Office, Bracknell.
Rowntree, P.R.	1983	Sensitivity of general circulation models to land surface processes. In proceedings of workshop on 'Inter-comparison of large-scale models for extended range forecasts', ECMWF, 1982, pp 225-261.
Rowntree, P.R.	1984	Review of general circulation models as a basis for predicting the effects of vegetation change on climate. Proceedings of the United Nations university workshop on 'Forests, climate and hydrology-regional impacts' at Oxford, March 1984.
Rutherford, M.C.,	1984	Relative allocation and seasonal phasing of growth of woody plant components in a South African savannah. Progress in Biometeorology, 3, 200-221.

Saker, N.J. 1975 An 11-layer general circulation model. Met O 20 Technical Note No II/30, Meteorological Office, Bracknell.

Shuttleworth, W.J. et al 1984 Eddy correlation measurements of energy partition for Amazonian forest. Quart. J. R. Met. Soc. 110, 1143-1162.

Slingo, J.M. 1979 A new interactive radiation scheme for the 5-level model. Met O 20 Technical Note No. II/135, Meteorological Office, Bracknell.

Slingo, J.M. 1982 A study of the earth's radiation budget using a general circulation model.

Quart. J.R. Met.Soc., 108, pp 379-405.

Street, F.A., and Grove, A.T. 1979 Global maps of lake-level fluctuations since 30,000 yr. B.P. Quat. Res. 12, 83-118.

Sud, Y.C. and Fennessy, M. 1982 A study of the influence of surface albedo on July circulation in semi-arid regions using the GLAS GCM.

J. Climatology 2, pp 105-125.

Walker, J. 1977 Interactive cloud and radiation in the 11-layer model Part 1: Radiation scheme.

Met O 20 Technical Note No II/91, Meteorological Office, Bracknell.

Walker, J. and Rowntree, P.R. 1977 The effect of soil moisture on circulation and rainfall in a tropical model.

Quart. J.R. Met. Soc., 103, pp 29-46.

Warren, A. and Maizels, J.K., 1977 Ecological change and desertification. In 'Desertification: its causes and consequences', (ed. Secretariat of the U.N. Conference on Desertification), Pergamon Press, pp 169-260.

Table 1

SPECIFIC HUMIDITIES (q) IN THE INITIAL ATMOSPHERE

Values shown are means over the area 10° - 32°N, 15°W - 35°E

LEVEL with σ at boundaries and mid-points		q g/kg	
		MOIST	'DRY'
.00			
1	.022	-.09	.001
.06			
2	.089	-.01	.001
.125			
3	.157	.02	.0035
.195			
4	.230	.03	.0097
.27			
5	.317	.37	.032
.37			
6	.436	1.18	.41
.51			
7	.578	3.15	1.5
.65			
8	.718	6.17	2.3
.79			
9	.844	10.36	5.4
.90			
10	.937	11.58	7.5
.975			
11	.987	11.81	7.5
1.0			

Table 2

SPECIFICATIONS OF THE EXPERIMENTS

Experiment number	Radiation scheme	Initial Saharan Conditions	
		atmosphere	soil
I1	Interactive	Moist	Dry
I2	Interactive	'Dry'	Dry
C1	Climatological	Moist	Dry
C2	Climatological	'Dry'	Dry
I3	Interactive	'Dry'	Moist
I4	Interactive	Moist	Dry*
C2a **	Climatological	'Dry'	Dry

* Soil kept dry in this region

** Surface albedo variation imposed over Africa

Table 3

MEANS FOR DAYS 7–16 AVERAGED OVER THE SAHARAN REGION 18°–32°N, 10°W–30°E

Radiation	Initial Saharan Atmosphere (experiment)	Soil Moisture Content cm	Rainfall mm day^{-1}	Evaporation mm day^{-1}	Sensible Heat Wm^{-2}	Sensible + Latent Heat Wm^{-2}	Atmospheric Water Content mm equivalent	Net Downward Radiation at top of Atmosphere (Day 16 only) Wm^{-2}
Interactive	Moist (I1)	0.32	1.92	1.63	81.8	128.9	33.78	63.7
	'Dry' (I2)	0.04	0.38	0.36	99.0	109.5	22.45	48.3
	'Dry' (I3)*	5.93	2.90	5.12	16.0	164.0	37.60	not available
	Moist (I4)**	0.00	0.84	0.00	108.7	108.7	25.95	not available
Climatological	Moist (C1)	0.45	2.82	2.36	102.4	170.6	34.43	62.8
	'Dry' (C2)	0.09	1.09	0.94	138.5	165.6	23.86	56.2
	'Dry' (C2a)***	0.06	0.84	0.73	123.5	144.5	23.17	43.7

* initial moist soil
** soil kept dry
*** albedo variation

TABLE 4

Mean temperatures (T) and specific humidities (q) for days 7-16 averaged over the Saharan region 18° - 32°N, 10°W - 30°E with interactive radiation and initial realistically dry Saharan atmosphere with soil initially dry (I2) and moist (I3).

	σ—	.987	.937	.844	.718	.578	.436	.317	.230	.157	.089	.022
T	I2	303.9	301.3	293.7	282.1	269.7	255.2	239.0	229.1	213.7	200.8	208.1
	I3	292.3	289.9	285.3	278.8	271.6	258.1	240.9	227.3	213.6	201.3	208.0
	I3 - I2	-11.6	-11.4	- 8.4	- 3.3	1.9	2.9	1.9	- 1.8	- 0.1	0.5	- 0.1
q	I2	6.31	6.07	5.56	4.11	2.64	0.95	0.21	0.03	0.00	0.00	0.00
	I3	13.03	11.25	9.60	7.00	3.07	1.37	0.37	0.05	0.00	0.00	0.00
	I3 - I2	6.72	5.18	4.04	2.89	0.43	0.42	0.16	0.02	0.00	0.00	0.00

FIGURE CAPTIONS

Figure 1 Saharan regions showing the areas over which changes were made to the initial conditions (10° - 32°N, 15°W - 35°E) and over which results are meaned (18° - 32°N, 10°W - 30°E). The dashed line indicates the boundary of initially dry soil.

Figure 2 Rainfall (mm/day) for a time mean of days 21-50 with interactive radiation (a) initial moist Saharan atmosphere (I1) (b) initial realistically dry Saharan atmosphere (I2). Stippling for values greater than 5mm/day.

Figure 3 Time series meaned over the Saharan region (18° - 32°N, 10°W - 30°E) for (a) soil moisture content (b) daily rainfall (c) atmospheric water content. Experiments defined in Table 2.

Figure 4 Difference in temperature (meaned over 10°W - 30°E) for a time mean of days 21-50 with interactive radiation: initial realistically dry Saharan atmosphere (I2) minus initial moist Saharan atmosphere (I1). Values are at 0000 GMT.

Figure 5 700 mb wind field for a time mean of days 21-50 with interactive radiation (a) initial moist Saharan atmosphere (I1) (b) initial realistically dry Saharan atmosphere (I2). Each full feather denotes 5 m/s.

Figure 6 (a) Zonal wind (meaned over 10°W - 30°E) for a time mean of days 21-50 with interactive radiation and initial moist Saharan atmosphere (I1) (b) as (a) but for initial realistically dry Saharan atmosphere (I2) (c) Observed cross section of June - August zonal mean wind at 20°E (Newell et al, 1972); solid contours at 10 ms^{-1} intervals (d), (e), (f). As (a), (b), (c) respectively, but for meridional wind; solid contours at 2 ms^{-1} intervals.

Figure 7 (a) Meridional wind (meaned over 10°W - 30°E) for a time mean of days 41-50 with interactive radiation and initial moist Saharan atmosphere (I1). Valid at 0000 GMT.
(b) As (a) but for 1200 GMT.
(c) As (a) but for a mean of 0000, 0600, 1200, and 1800 GMT.
(d), (e), (f) As (a), (b), (c) respectively, but for initial realistically dry atmosphere (I2).

Figure 8 Meridional wind (meaned over 10°W - 30°E) for a time mean of days 21-50 with interactive radiation at 0000 GMT. Realistically dry minus moist initial Saharan atmosphere (I2 - I1).

Figure 9 200 mb zonal wind (m/s) for a time mean of days 21-50 with interactive radiation. (a) initial realistically dry Saharan atmosphere (I2). Light stippling for westerlies greater than 20 m/s and heavy stippling for easterlies greater than 20 m/s. (b) dry minus moist initial Saharan atmosphere (I2 - I1). Light stippling for increases of more than 5 m/s and heavy stippling for decreases of more than 5 m/s.

Figure 10 Northward moisture flux (meaned over 10°W - 30°E) for a time mean of days 41-50 using six-hourly data (a) initial moist Saharan atmosphere (I1) (b) initial realistically dry Saharan atmosphere (I2). Units of 0.01 m/s.

Figure 11 Vertically integrated northward moisture flux (meaned over $10^{\circ}W - 30^{\circ}E$) for a time mean of days 41-50 using six-hourly data for experiments I1 and I2.

Figure 12 (a) Vertical velocity (mb/day) at 500 mb for a time mean of days 41-50 with interactive radiation and initial realistically dry Saharan atmosphere (I2). Valid at 0000 GMT. Ascent negative. Light stippling for descent greater than 50mb/day and heavy stippling for ascent greater than 50mb/day.
(b) As (a) but for 1200 GMT.
(c) As (a) but for a mean of 0000, 0600, 1200 and 1800 GMT with initial moist Saharan atmosphere (I1).
(d) As (c) but for initial realistically dry Saharan atmosphere. (I2).

Figure 13 Rainfall (mm/day) for a time mean of days 7-16 with interactive radiation and initial realistically dry Saharan atmosphere with soil initially (a) dry (I2) (b) moist (I3). Stippling for values greater than 5mm/day.

Figure 14 Geographical distribution of albedo used in experiment C2a.

Figure 15 Rainfall for a time mean of days 7-16 zonally-averaged over Africa and Arabia in the experiment which started from the realistically dry Saharan atmosphere and used climatological radiation.

Figure 16 Rainfall and albedo differences for a time mean of days 7-16 zonally averaged over Africa and Arabia with a varying albedo. Experiments C2a minus C2.

Figure 17 Rainfall (mm/day) for a time mean of days 7-16 in the experiments which started from the realistically dry Saharan atmosphere and used climatological radiation (a) C2 (constant albedo) with stippling for values greater than 5mm/day (b) C2a (varying albedo) minus C2. with light stippling for increases of more than 2mm/day and heavy stippling for decreases of more than 2mm/day.

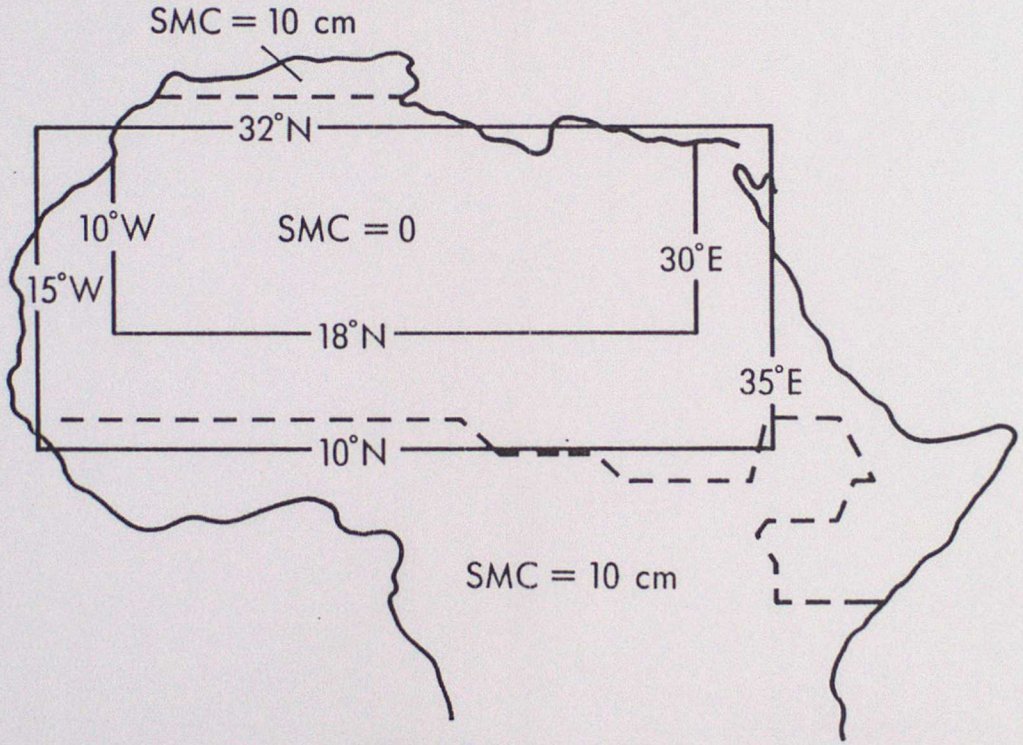

Figure 1

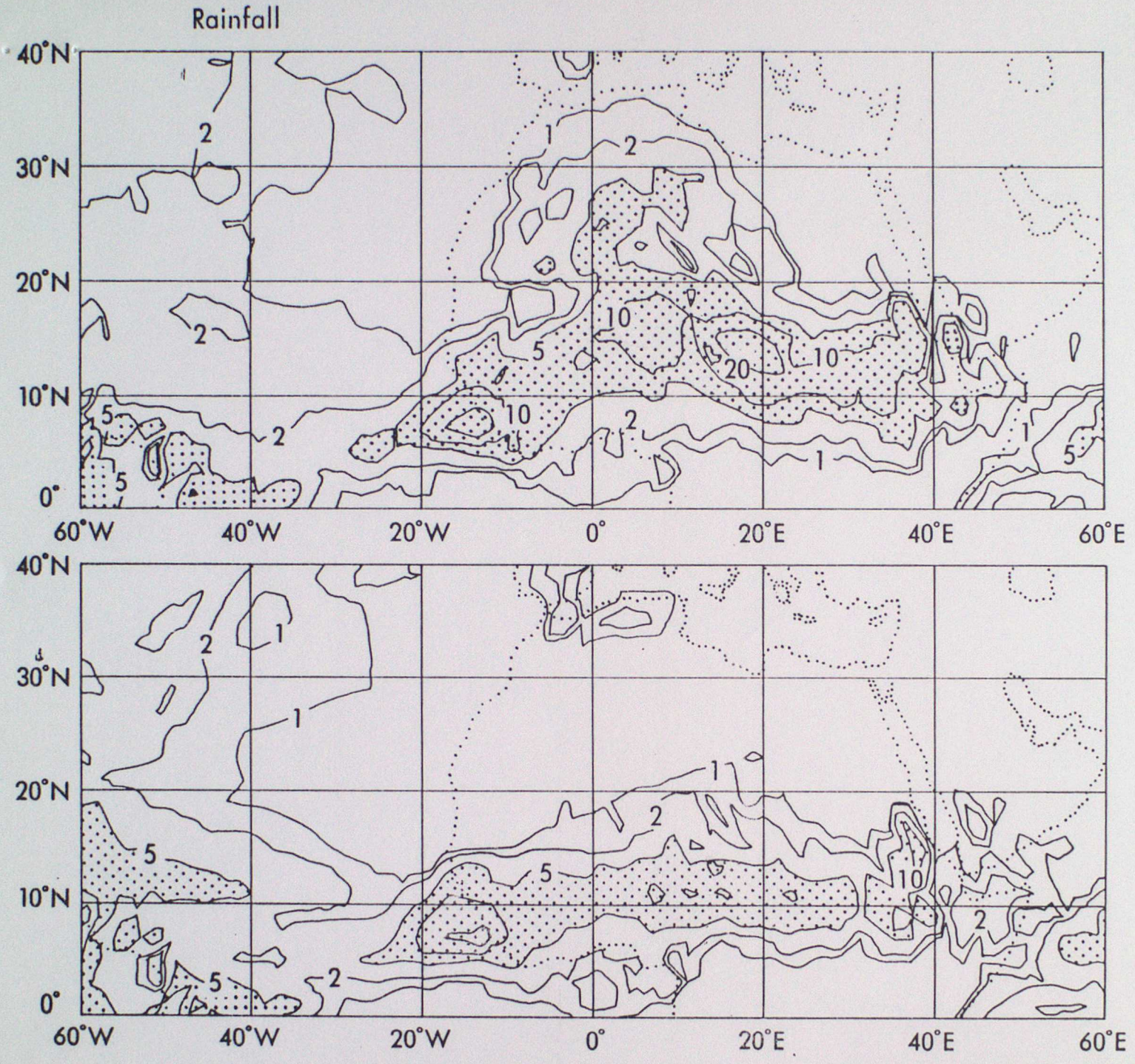

Figure 2

(a) Soil moisture content

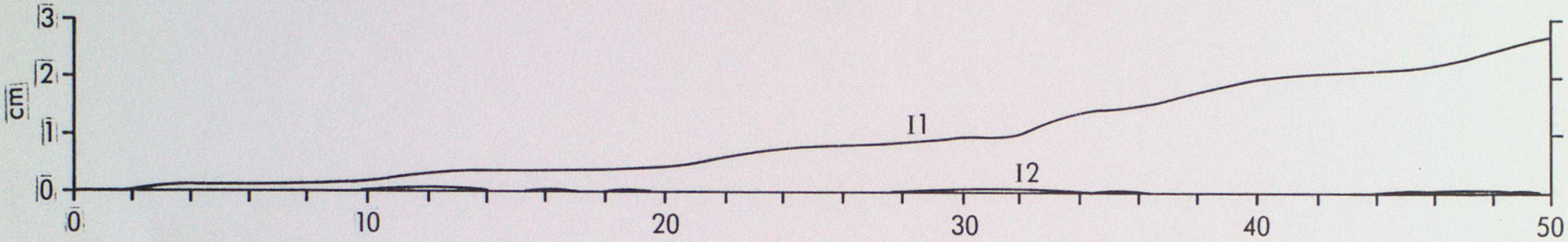

(b) Daily rainfall

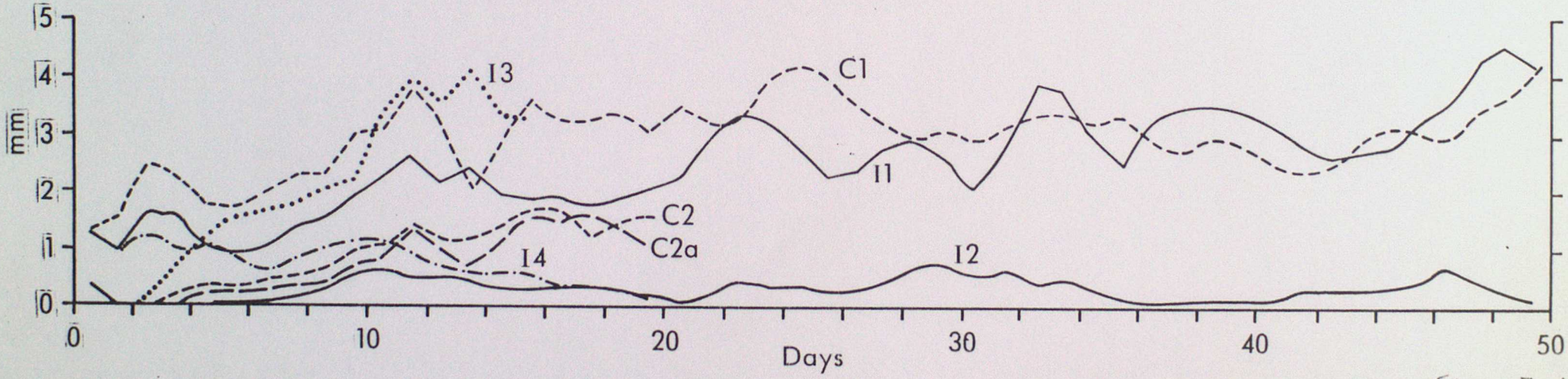

Figure 3 (a,b)

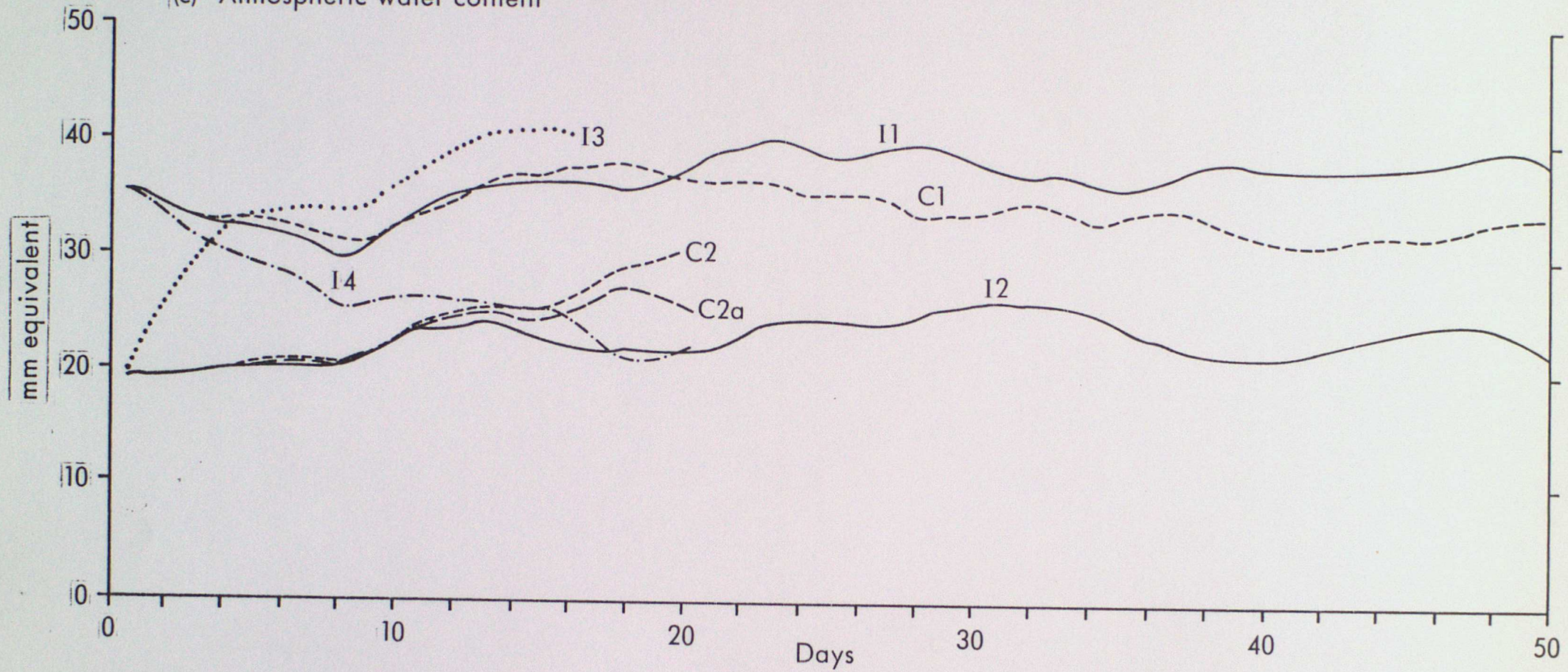
(c) Atmospheric water content
mm equivalent
50
40
30
20
10
0
0
10
20
30
40
50
Days
I3
I1
C1
C2
I4
C2a
I2

Figure 3(c)

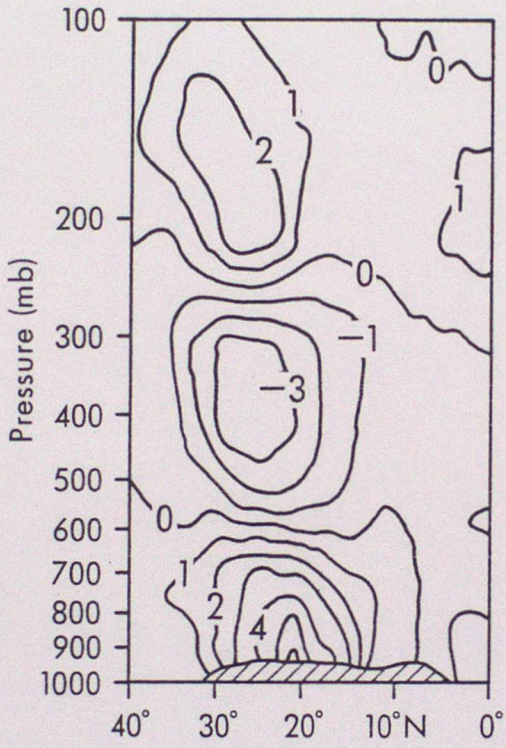
Pressure (mb)
100
200
300
400
500
600
700
800
900
1000
40°
30°
20°
10°N
0°
0
1
2
0
1
0
−1
−3
0
1
2
4

Figure 4

700-MB Winds

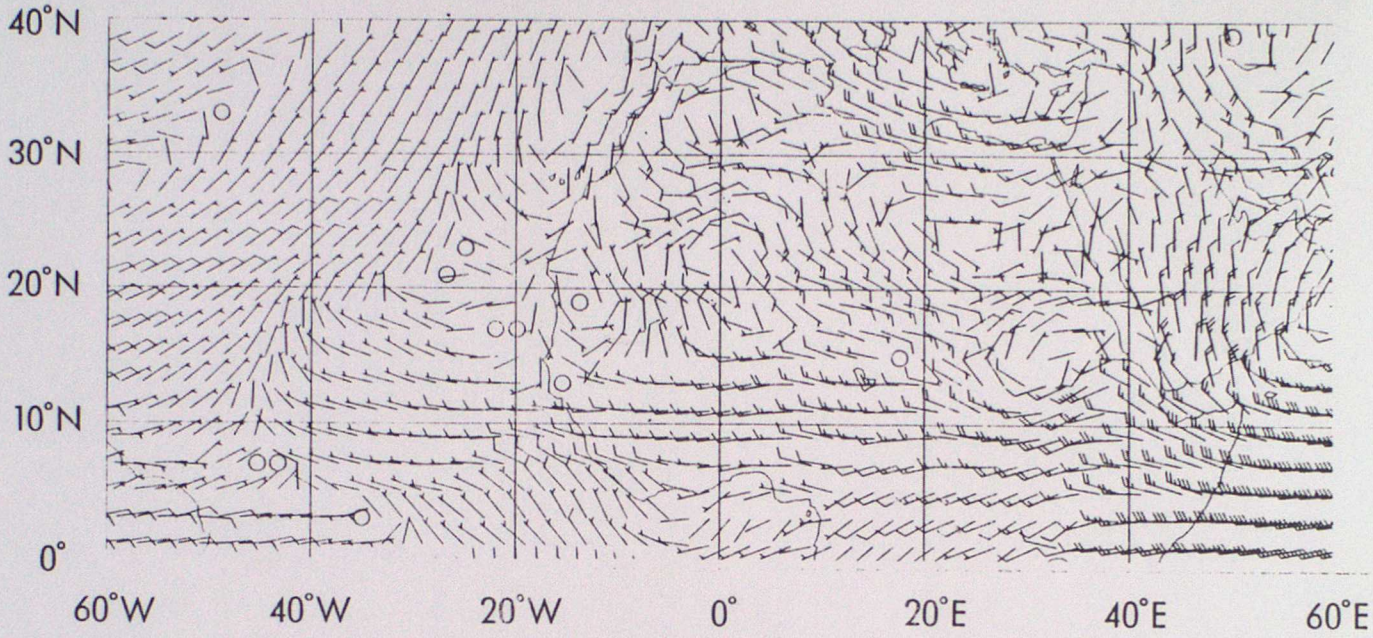

(a) I1

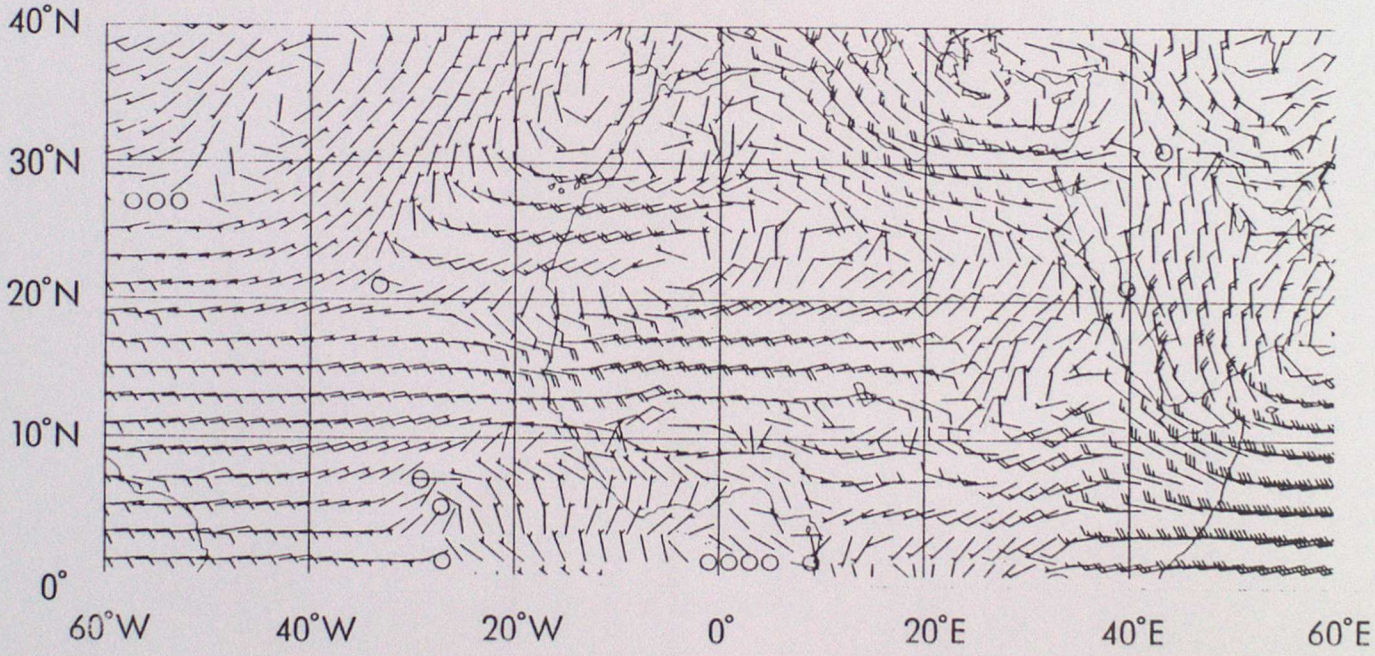

(b) I2

Figure 5

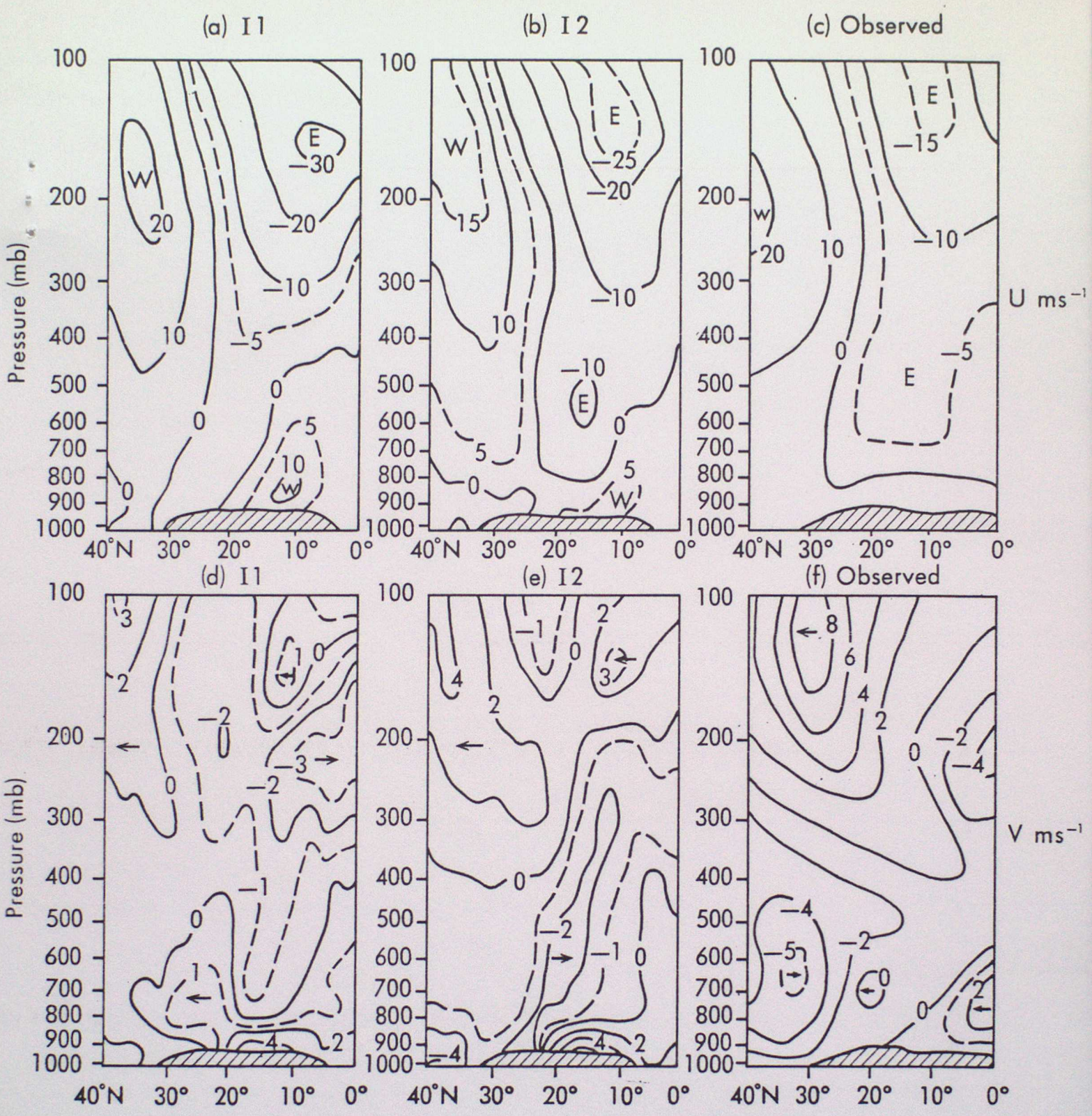
(a) I1
(b) I2
(c) Observed
(d) I1
(e) I2
(f) Observed
Pressure (mb)
100
200
300
400
500
600
700
800
900
1000
40°N
30°
20°
10°
0°
U ms⁻¹
V ms⁻¹
W
E

Figure 6

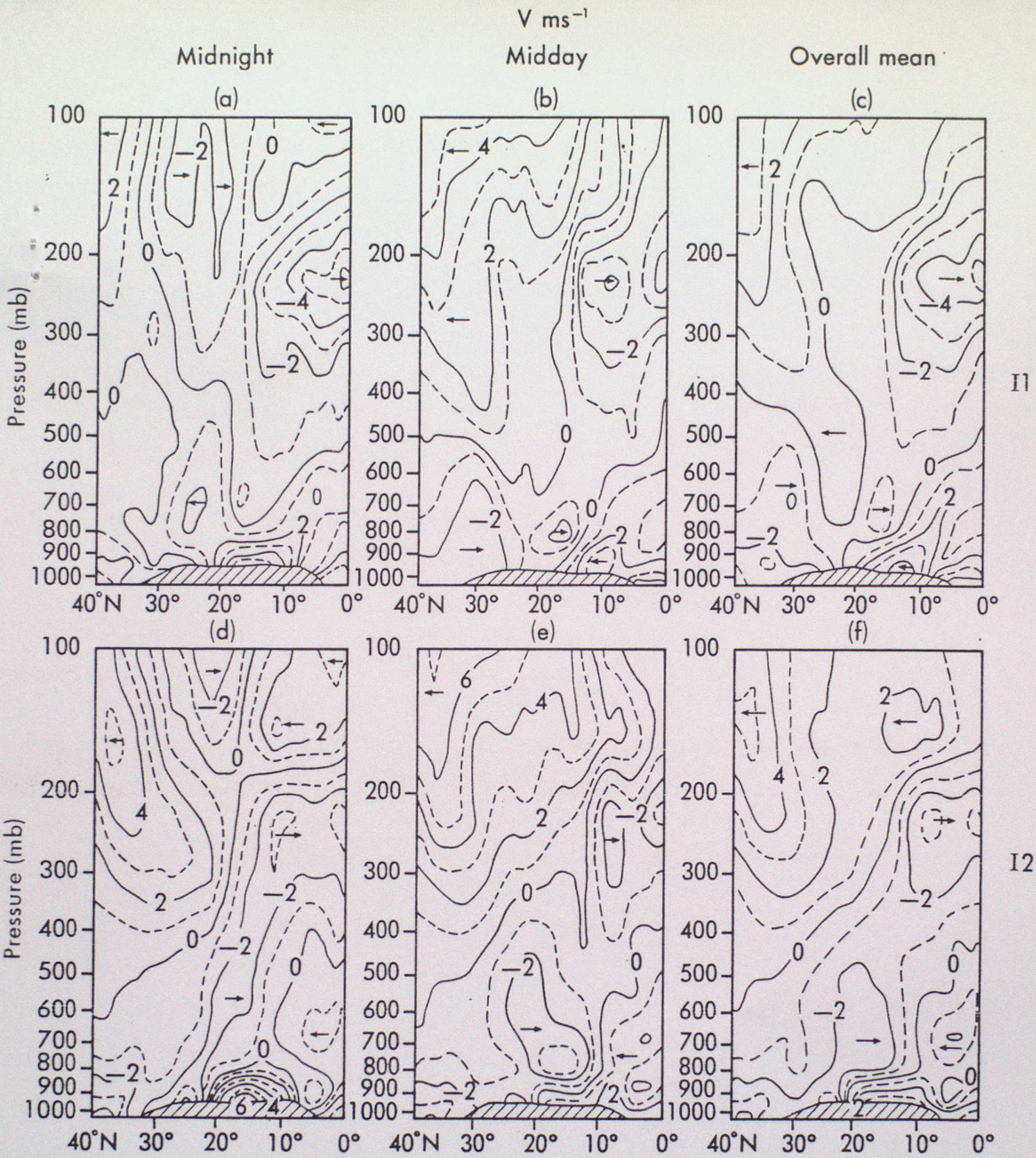
V ms⁻¹
Midnight
Midday
Overall mean
(a)
(b)
(c)
(d)
(e)
(f)
Pressure (mb)
100
200
300
400
500
600
700
800
900
1000
40°N
30°
20°
10°
0°
I1
I2

Figure 7

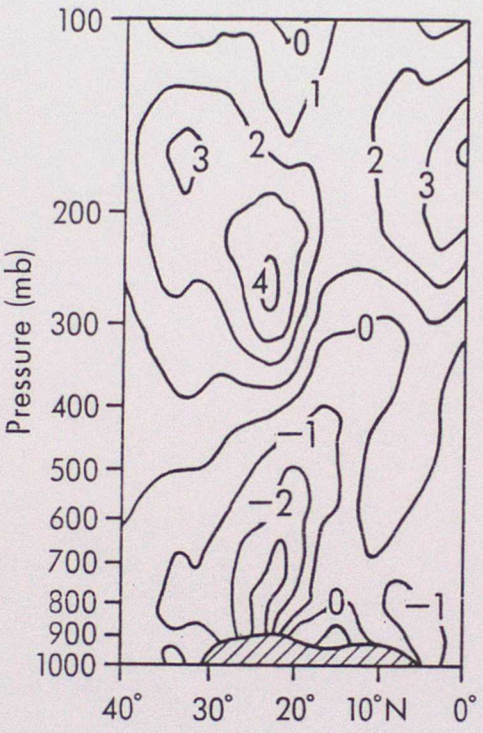
Pressure (mb)
100
200
300
400
500
600
700
800
900
1000
40°
30°
20°
10°N
0°
0
1
2
3
4
2
3
0
−1
−2
0
−1

Figure 8

(a) I2

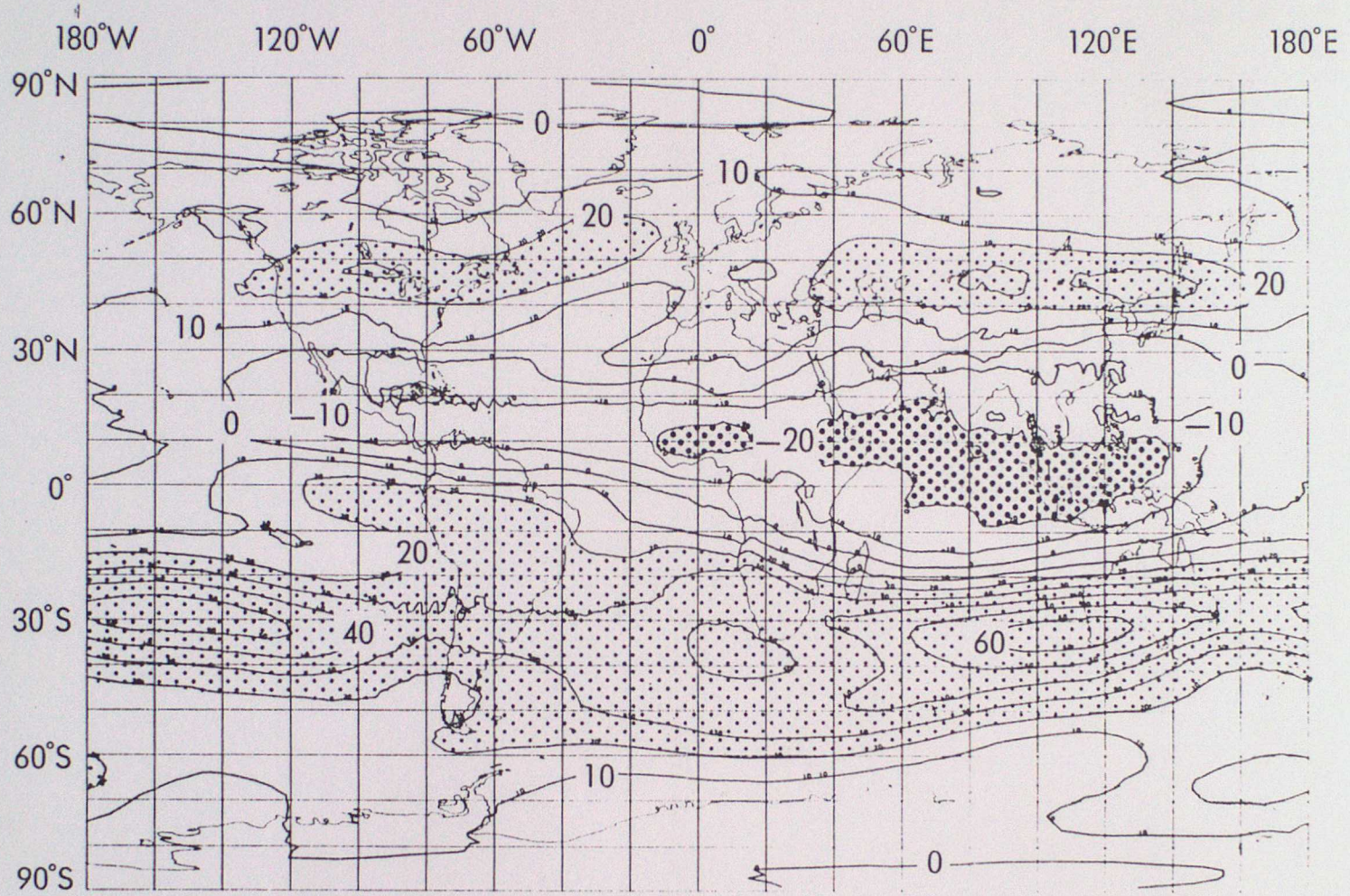

Figure 9 (a)

(b) 12—11

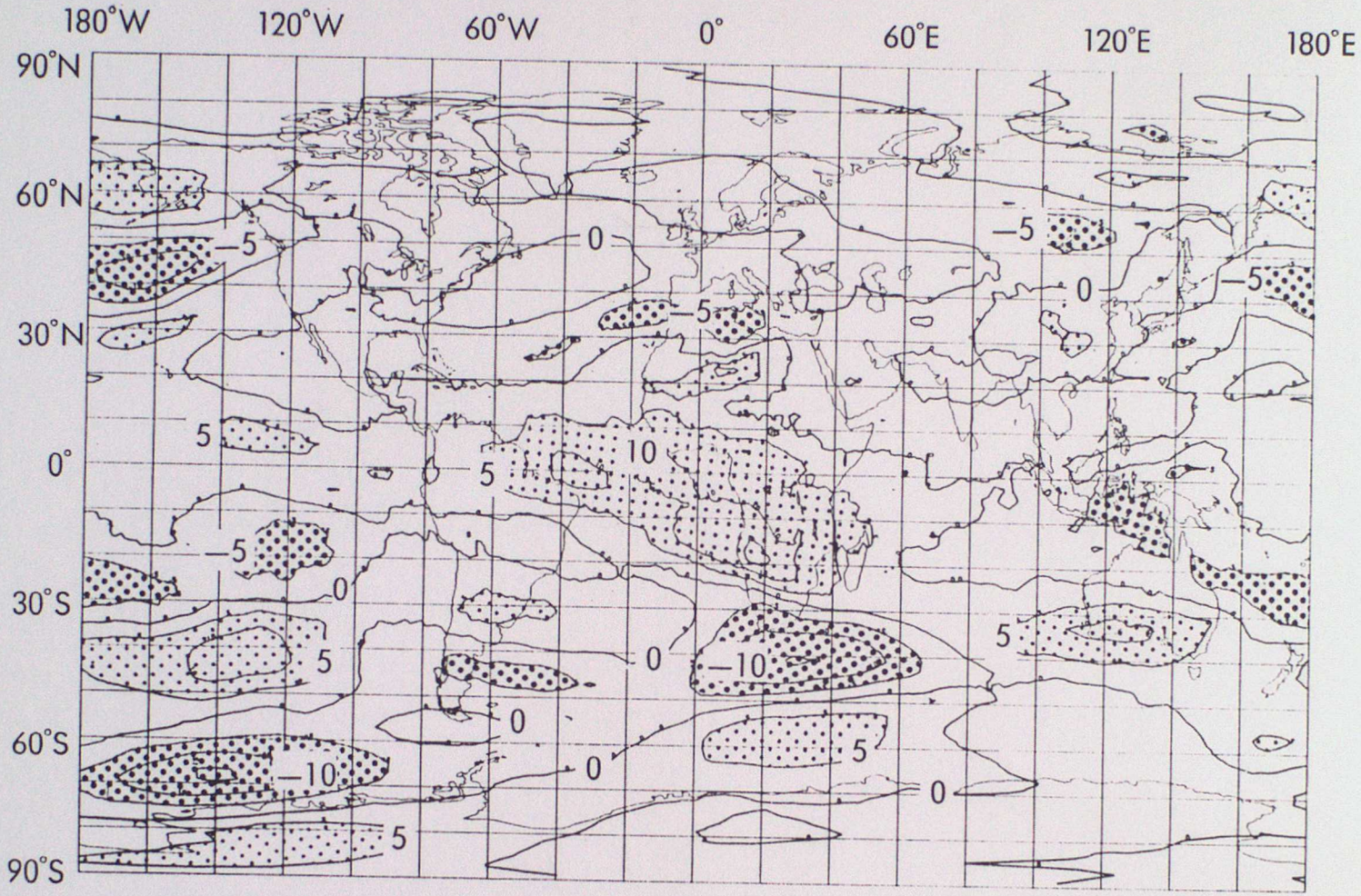

Figure 9(b)

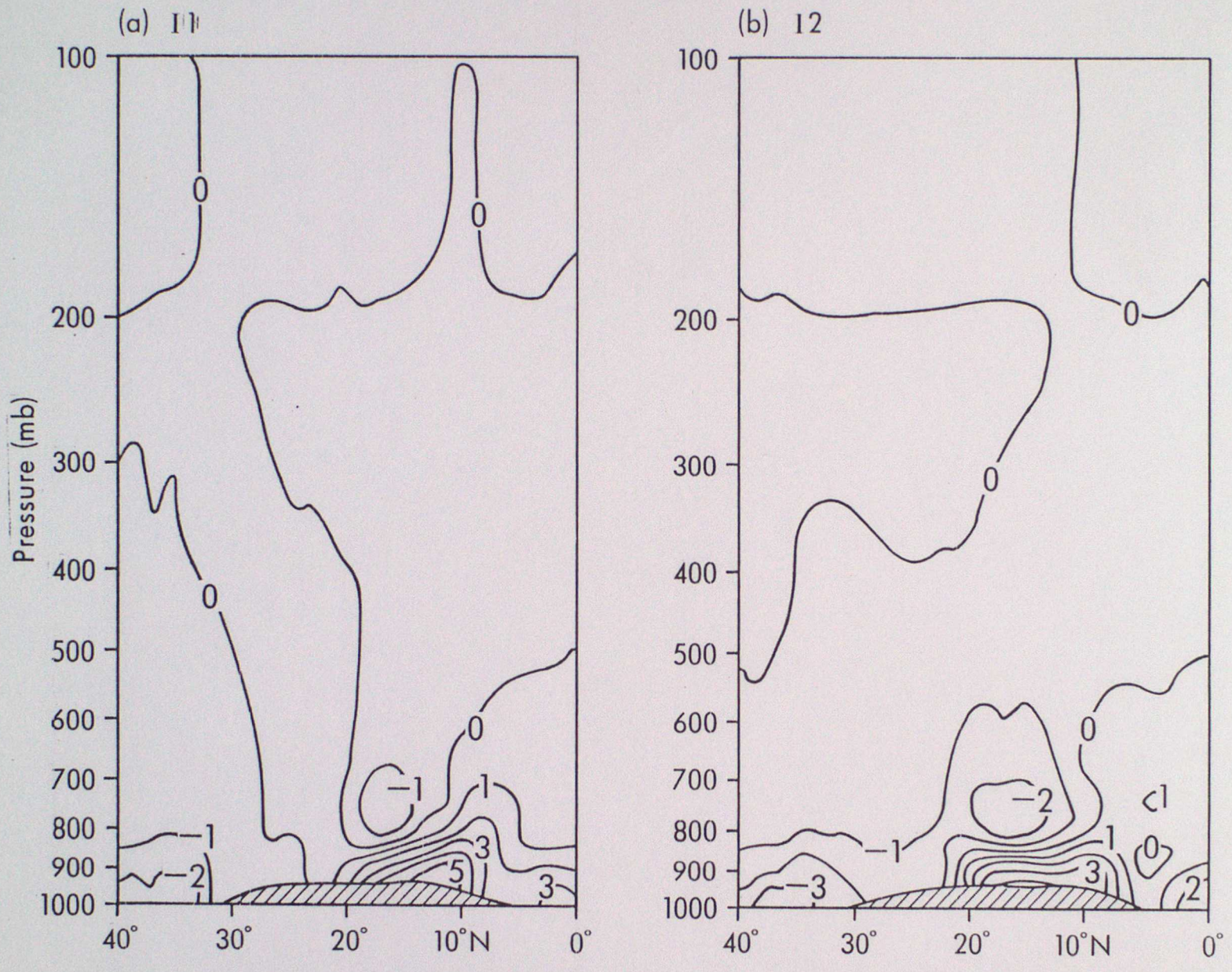
(a) I1
(b) I2
Pressure (mb)
100
200
300
400
500
600
700
800
900
1000
40°
30°
20°
10°N
0°
0
-1
-2
-3
1
3
5
<1

Figure 10

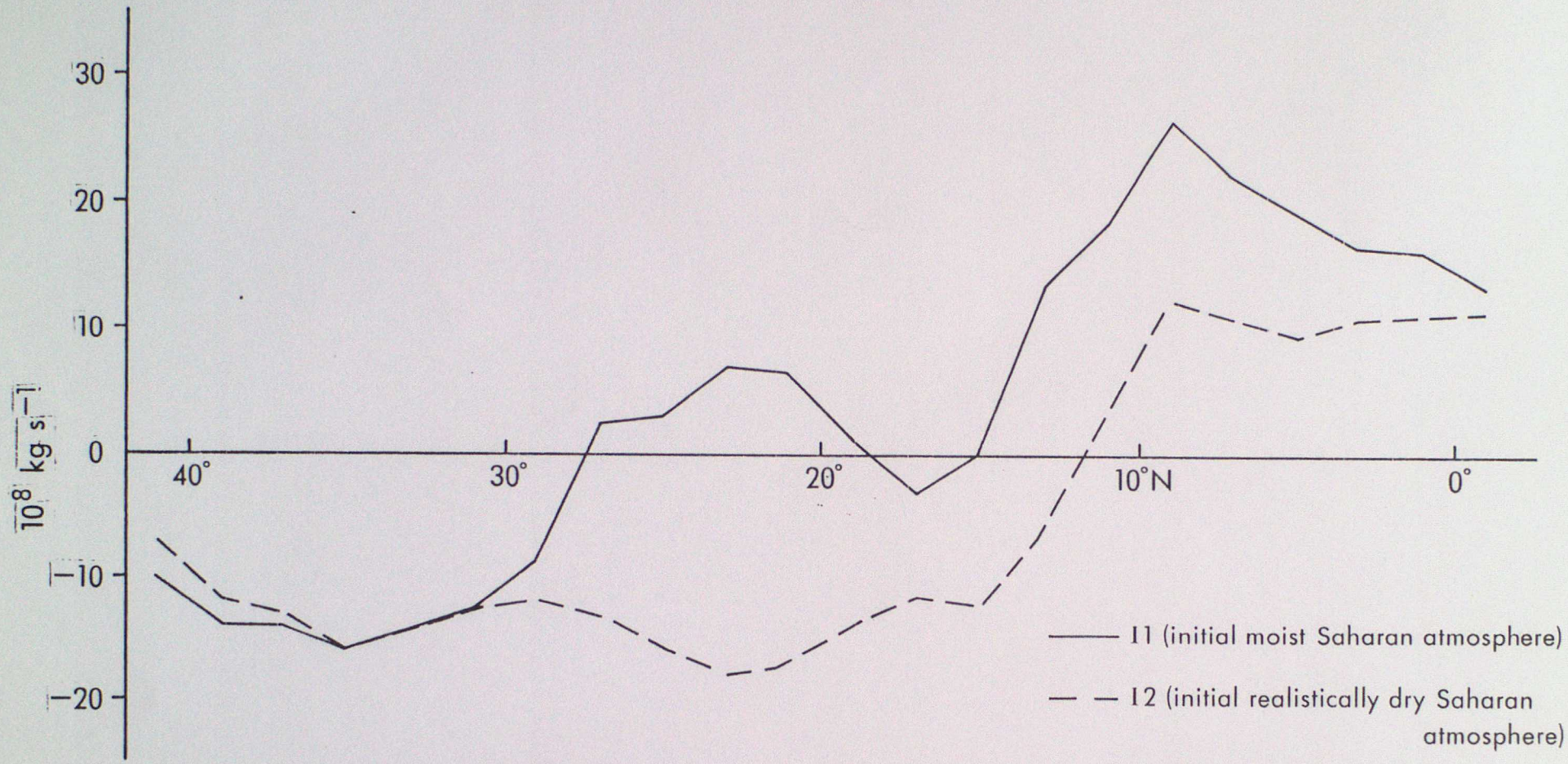
30
20
10
0
−10
−20
10^8 kg s^{-1}
40°
30°
20°
10°N
0°
I1 (initial moist Saharan atmosphere)
I2 (initial realistically dry Saharan atmosphere)

Figure 11

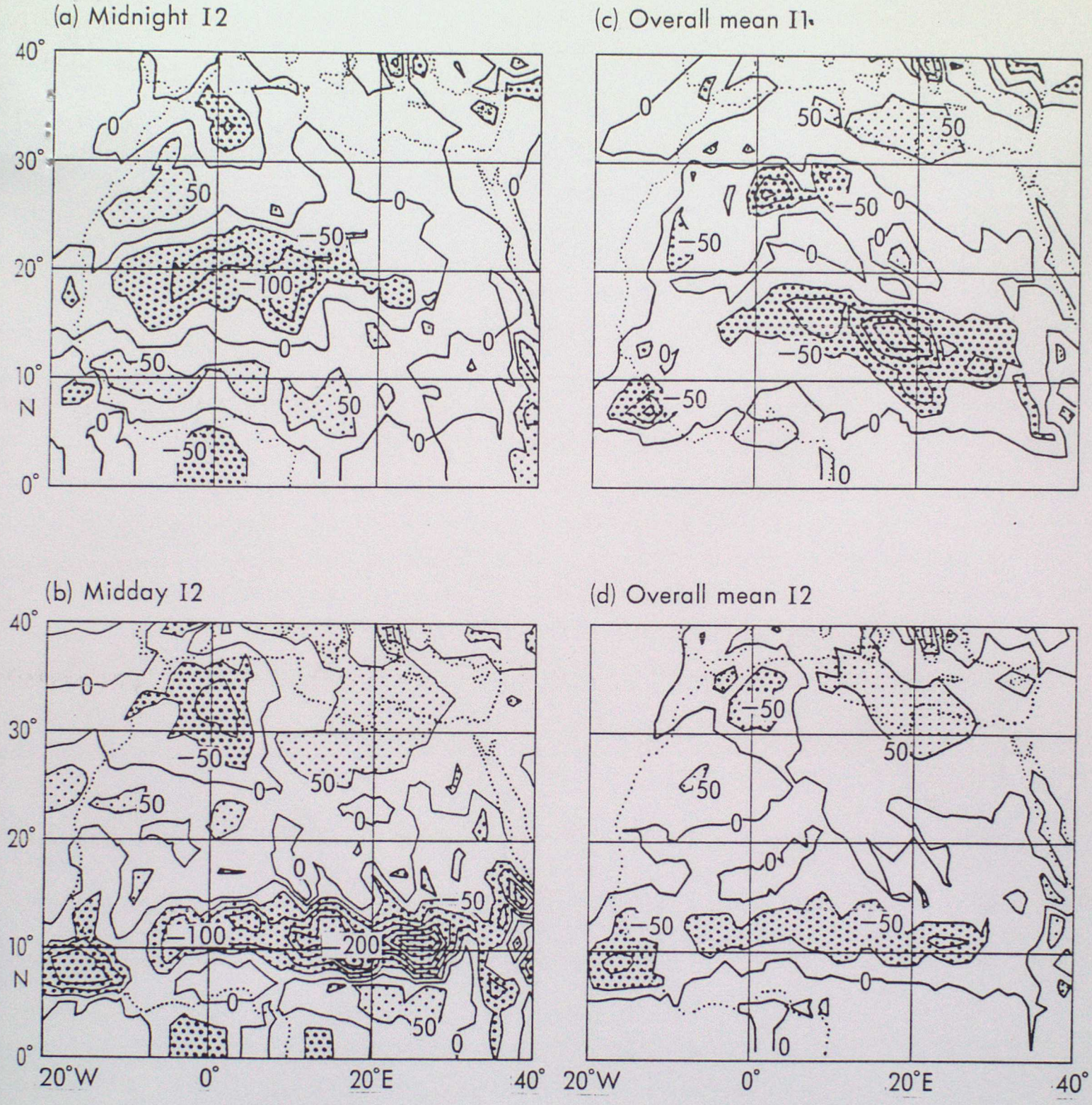
(a) Midnight I2
(c) Overall mean I1
(b) Midday I2
(d) Overall mean I2
40°
30°
20°
10°
N
0°
20°W
0°
20°E
40°
0
50
−50
−100
−200

Figure 12

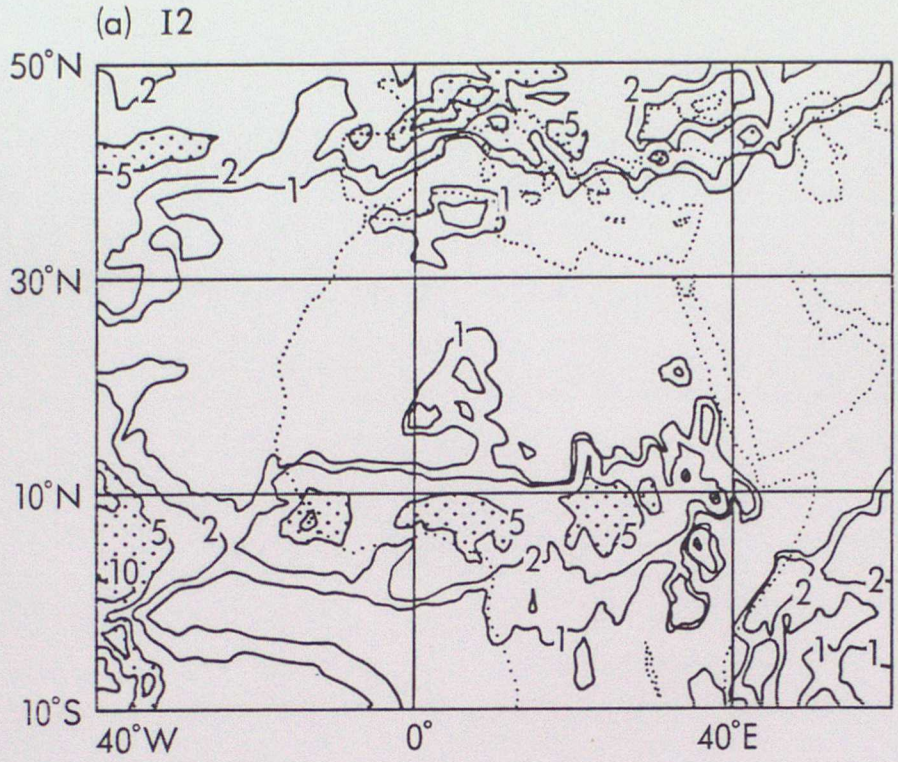

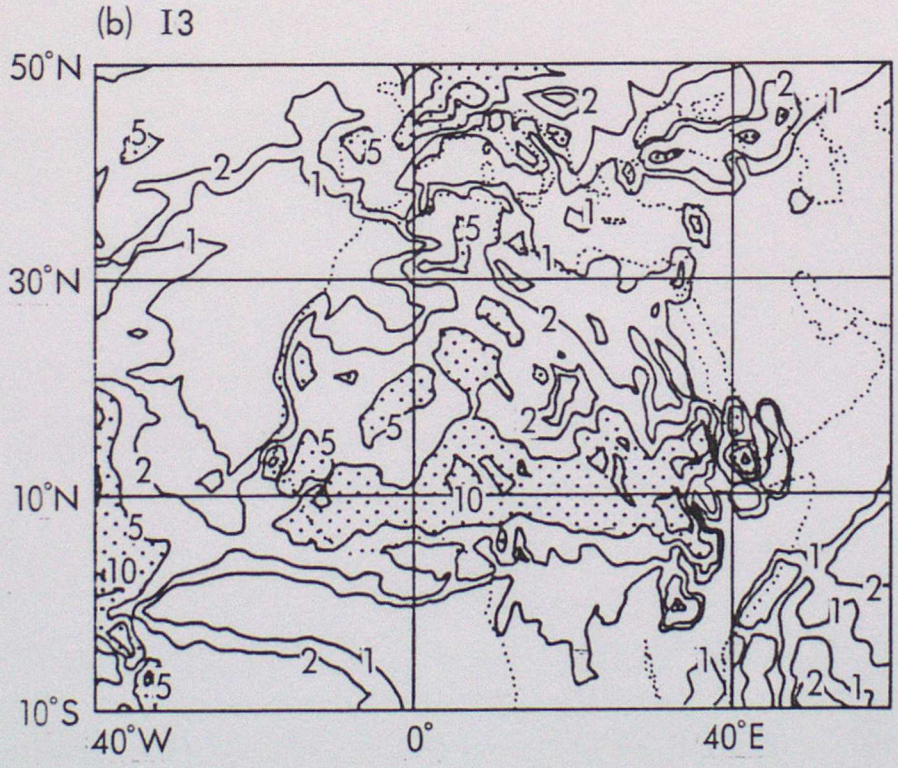

Figure 13

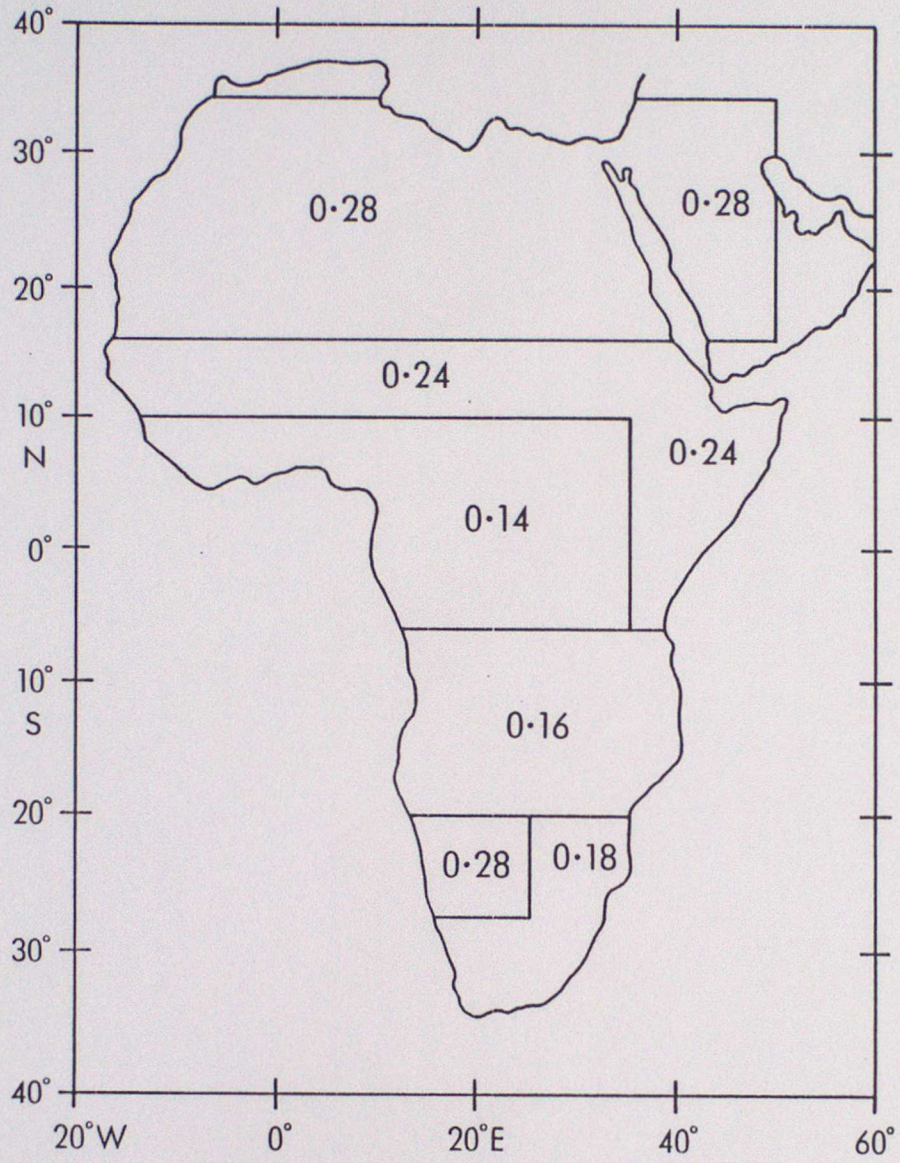
40°
30°
20°
10°
N
0°
10°
S
20°
30°
40°
20°W
0°
20°E
40°
60°
0·28
0·28
0·24
0·24
0·14
0·16
0·28
0·18

Figure 14

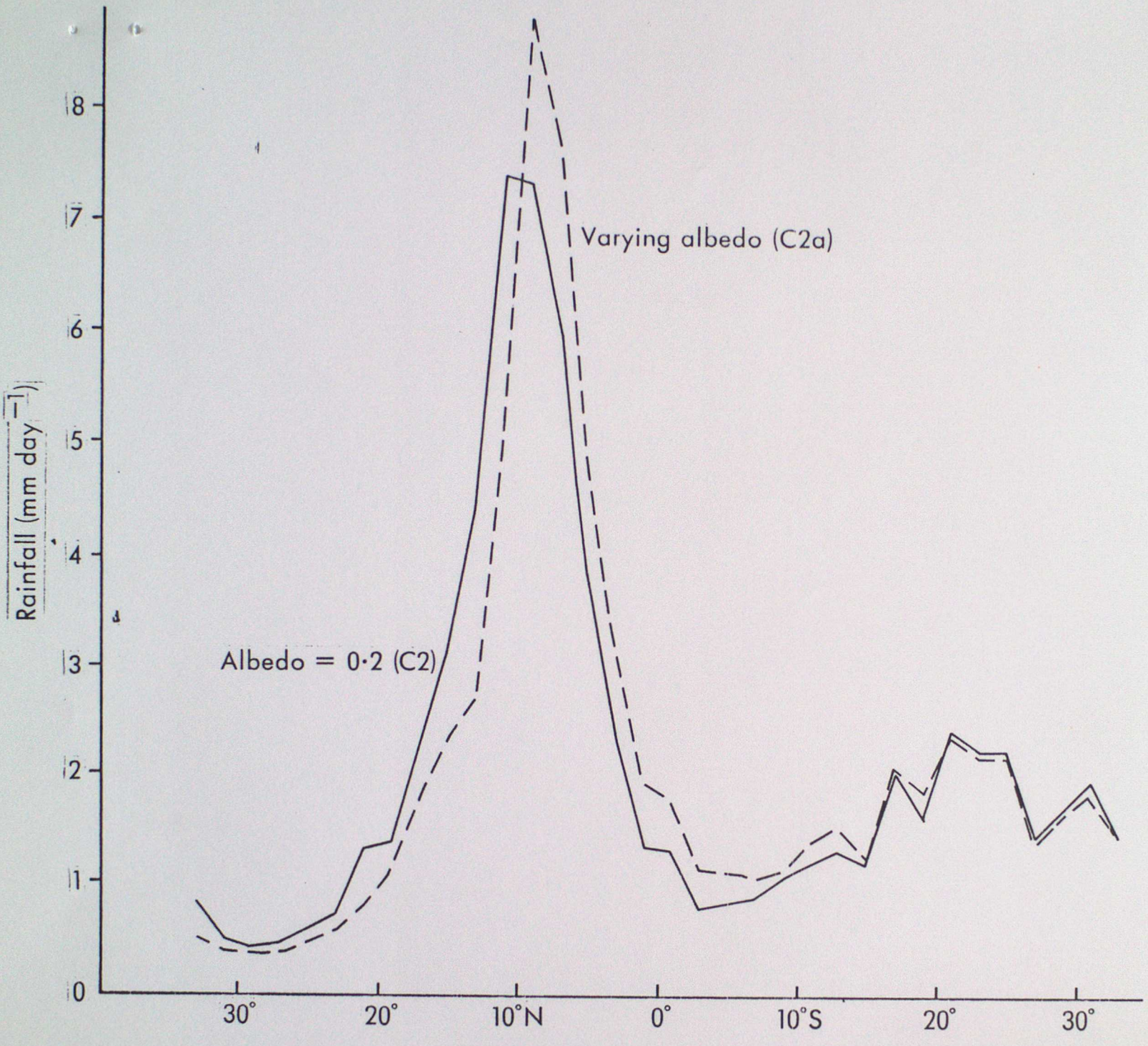
Rainfall (mm day⁻¹)
8
7
6
5
4
3
2
1
0
Varying albedo (C2a)
Albedo = 0·2 (C2)
30°
20°
10°N
0°
10°S
20°
30°

Figure 15

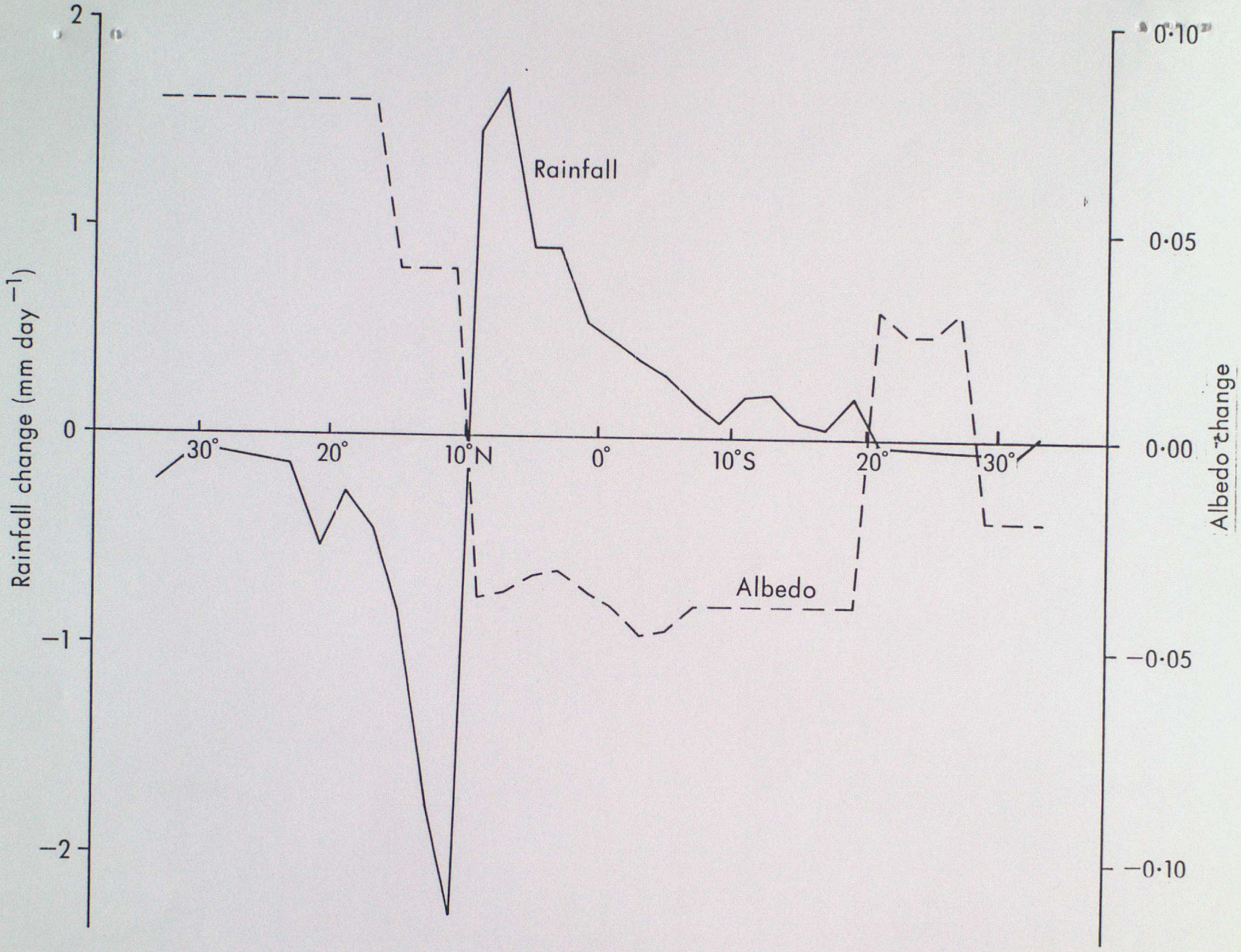
2
1
0
−1
−2
Rainfall change (mm day^{-1})
0·10
0·05
0·00
−0·05
−0·10
Albedo change
30°
20°
10°N
0°
10°S
20°
30°
Rainfall
Albedo

Figure 16

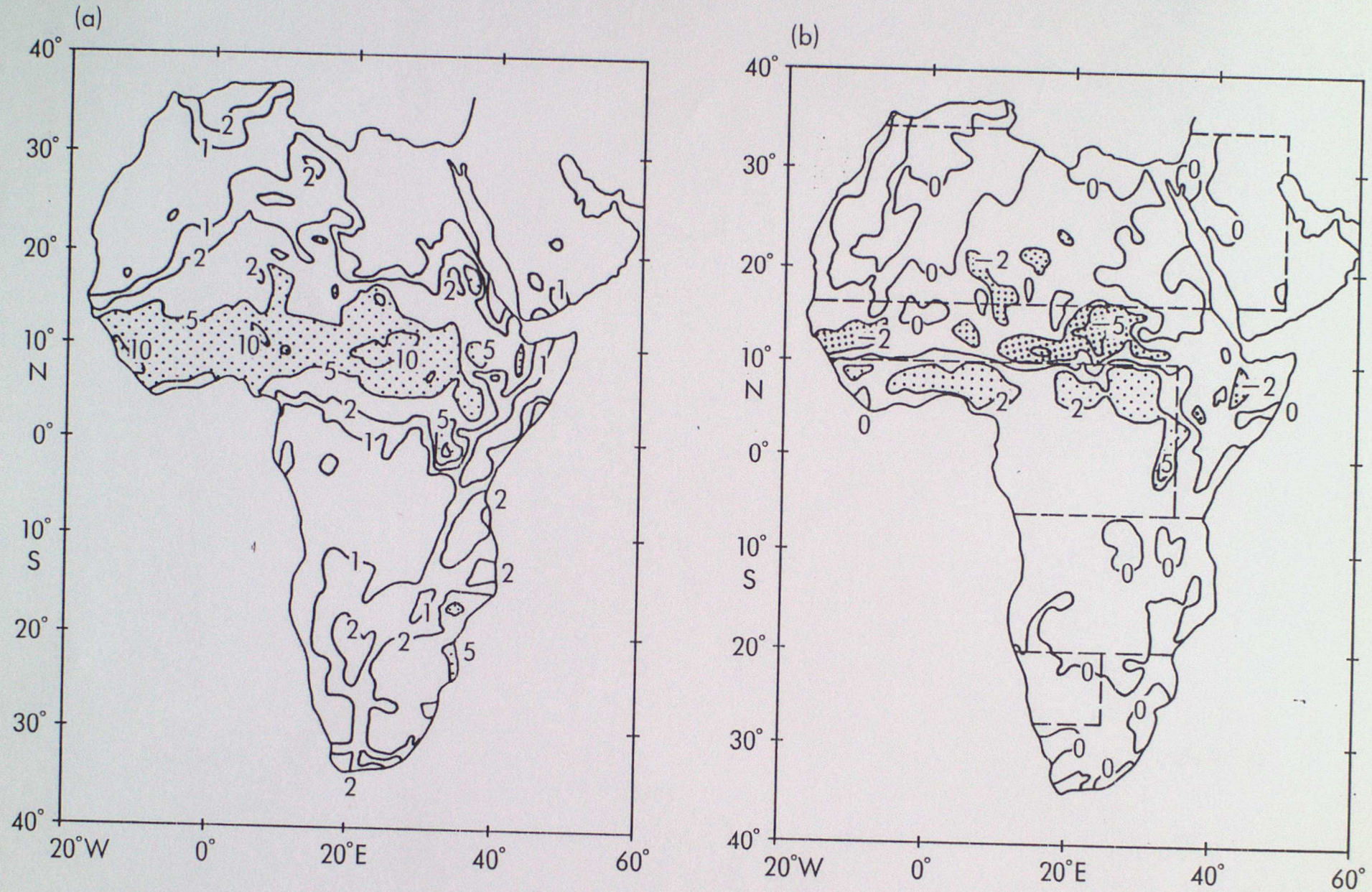

Figure 17